

# **TECHNICAL REPORT 95-05**

## **A Quantitative Mechanistic Description of Ni, Zn and Ca Sorption on Na-Montmorillonite**

### **Part II: Sorption Measurements**

July 1995

B. Baeyens, M.H. Bradbury

PSI, Würenlingen and Villigen



# **TECHNICAL REPORT 95-05**

## **A Quantitative Mechanistic Description of Ni, Zn and Ca Sorption on Na-Montmorillonite**

### **Part II: Sorption Measurements**

July 1995

B. Baeyens, M.H. Bradbury

PSI, Würenlingen and Villigen

This report was prepared on behalf of Nagra. The viewpoints presented and conclusions reached are those of the author(s) and do not necessarily represent those of Nagra.

"Copyright © 1995 by Nagra, Wettingen (Switzerland) / All rights reserved.

All parts of this work are protected by copyright. Any utilisation outwith the remit of the copyright law is unlawful and liable to prosecution. This applies in particular to translations, storage and processing in electronic systems and programs, microfilms, reproductions, etc. "

## **PREFACE**

The Laboratory for Waste Management at the Paul Scherrer Institut is performing work to develop and test models as well as to acquire specific data relevant to performance assessments of Swiss nuclear waste repositories. These investigations are undertaken in close co-operation with, and with the financial support of, the National Cooperative for the Disposal of Radioactive Waste (Nagra). The present report is issued simultaneously as a PSI-Bericht and a Nagra Technical Report.



## **FOREWORD**

This report is the second in a series of three, which together describe experimental investigations and modelling studies on the sorption of radionuclides by Na-montmorillonite. The aim of this work was to identify sorption mechanisms, develop mass action based models and determine the associated parameter values. In Part I the conditioning (purifying) procedures applied to the source material (SWy-1 Na-montmorillonite) are given together with characterisation and titration results. Sorption edge and isotherm data for Ni, Zn and Ca are presented in Part II. In a final report, Part III, an overall model was developed to describe the acid/base and sorption behaviour on Na-montmorillonite.

## **VORWORT**

Der vorliegende Bericht ist der zweite aus einer Reihe von drei Berichten, die insgesamt die experimentellen Untersuchungen und Modellrechnungen zur Sorption von Radionukliden auf Na-Montmorillonit beschreiben. Ziel dieser Arbeit ist neben der Abklärung von Sorptionsmechanismen die Entwicklung von auf Massenwirkungsgesetzen basierenden Modellen und die Bestimmung der dazugehörigen Parameter. In Teil I werden Konditioniermethoden vorgestellt, mit Hilfe derer das Ausgangsmaterial (SWy-1 Na-Montmorillonit) aufgearbeitet wurde. Daneben werden Analysendaten und Ergebnisse der Titrations vorgest. Teil II behandelt die pH-abhängige Sorption und Sorptionsisotherme von Ni, Zn und Ca. In Teil III wird abschliessend ein umfassendes Modell vorgestellt, welches neben dem Säure/Base-Verhalten der Oberflächengruppen auch die Sorptionseigenschaften von Na-Montmorillonit beschreibt.

## **PRÉFACE**

Ce rapport est le deuxième d'une série de trois rapports qui décrivent les travaux expérimentaux et le développement d'une modélisation concernant la sorption de radionucléides par la montmorillonite sodique conditionnée. Le travail présenté ici se focalise sur l'identification des mécanismes de sorption, le développement d'un modèle et la détermination des paramètres associés. Dans le premier rapport on décrit un procédé de conditionnement du matériel de base, la montmorillonite sodique (SWy-1), et, les données de caractérisation et de titration. Dans le deuxième rapport, les seuils de sorption et les isothermes de sorption qui ont été déterminés pour le Ni, le Zn et le Ca sont décrits. Dans le troisième rapport, un modèle est présenté qui reflète uniquement le comportement acide/base des sites de surface et la sorption sur la montmorillonite sodique conditionnée.

**ABSTRACT**

The main focus of the experimental work presented here is the sorption behaviour of Ni on conditioned Na-montmorillonite. Ca and Zn were also studied as important background impurity cations which can, depending on the circumstances, be competitive for the available sorption sites. Distribution ratios were measured for all three radionuclides at trace concentrations as a function of pH over a range from 2 to 10.5 to produce so-called "sorption edges". In the cases of Ca and Ni such measurements were carried out as a function of the NaClO<sub>4</sub> background electrolyte concentration.

From the form of the sorption edges it was deduced that two main mechanisms were controlling the uptake of radionuclides onto the solid; a pH independent component, identified as cation exchange, and a pH dependent process interpreted as surface complexation on  $\equiv\text{SOH}$  type sites.

In addition to sorption edges, sorption isotherms were determined for Ni and Zn in solutions of 0.1 M NaClO<sub>4</sub> at several pH values. The non-linear sorption isotherms indicated that in addition to cation exchange, at least 2 different  $\equiv\text{SOH}$  type sites were present in Na-montmorillonite contributing to the overall sorption.

## ZUSAMMENFASSUNG

Der Schwerpunkt der in diesem Bericht dargestellten Arbeiten liegt auf der Untersuchung der Sorption von Ni auf konditioniertem Na-Montmorillonit. Im weiteren wurde das Sorptionsverhalten von Ca und Zn untersucht. Diese Metall-kationen treten als Verunreinigungen auf und können je nach Wahl der chemischen Bedingungen mit Ni um verfügbare Oberflächengruppen konkurrieren. Zur Bestimmung der pH-abhängigen Sorption wurden die Verteilungsverhältnisse für Ni, Zn und Ca im Spurenkonzentrationsbereich als Funktion des pH-Wertes (2 bis 10.5) gemessen. Für Ca und Ni wurden die Verteilungsverhältnisse zudem bei verschiedenen Hintergrundkonzentration des NaClO<sub>4</sub>-Elektrolyt bestimmt.

Aus der pH-Abhängigkeit der Sorption der Radionuklide geht hervor, dass zwei Hauptmechanismen vorliegen: ein pH-unabhängiger Prozess, der als Kationenaustausch identifiziert wurde, und ein pH-abhängiger Prozess, der als Komplexierung durch ≡SOH-Oberflächengruppen interpretiert wurde.

Zusätzlich zur pH-abhängigen Sorption wurden Sorptionsisothermen für Ni und Zn in einer 0.1 M NaClO<sub>4</sub> Lösung bei verschiedenen pH-Werten gemessen. Die Nichtlinearität der Sorptionsisothermen deutet darauf hin, dass neben den Kationenaustauschplätzen noch mindestens zwei verschiedene ≡SOH-Gruppen an der Oberfläche von Na-Montmorillonit vorhanden sind und zur Gesamtsorption der Radionuklide beitragen.

## RÉSUMÉ

Le travail expérimental présenté ici a été focalisé sur l'étude du comportement de sorption du Ni sur de la montmorillonite sodique conditionnée. Le Ca et le Zn ont aussi été étudiés, comme d'impuretés résiduelles importantes, car ils peuvent, suivant les circonstances, avoir un comportement compétitifs sur les sites de sorption présents. Les coefficients de distribution ont été mesurés pour les trois radionucléides, en concentration trace, en fonction du pH, pour des valeurs allant de 2 à 10.5, ce qui a permis de définir les seuils de sorption. Pour le Ca et le Ni, les mesures ont été faites en fonction de la concentration en électrolytique ( $\text{NaClO}_4$ ) du milieu.

La forme des seuils de sorption a permis de déduire que deux mécanismes principaux contrôlant la sorption de radionucléides sur le solide; un processus indépendant du pH, identifié comme échange cationique, et un processus dépendant du pH interprété comme une complexation de surface sur les sites du type  $\equiv\text{SOH}$ .

En plus des seuils de sorption, des isothermes de sorption ont été déterminées pour le Ni et le Zn dans des solutions de 0.1 M de  $\text{NaClO}_4$  à différents pH. La non-linéarité des isothermes de sorption indique qu'en plus de l'échange cationique, au moins deux sites différents de type  $\equiv\text{SOH}$ , contribuant à la sorption totale, sont présents dans la montmorillonite sodique.

**TABLE OF CONTENTS**

FOREWORD.....	I
VORWORT .....	I
PRÉFACE .....	I
ABSTRACT .....	II
ZUSAMMENFASSUNG .....	III
RÉSUMÉ .....	IV
TABLE OF CONTENTS .....	V
LIST OF FIGURES .....	VII
LIST OF TABLES.....	IX
1 INTRODUCTION.....	1
1.1 General .....	1
1.2 Background .....	1
2 MATERIALS AND METHODS .....	7
2.1 Na-montmorillonite .....	7
2.2 Radiotracers .....	7
2.3 Analytical Methods .....	7
2.4 Experimental Procedures.....	8
2.4.1 Sorption Edge Determinations .....	8
2.4.2 Isotherm Determinations .....	9
3 EXPERIMENTAL TECHNIQUES.....	10
3.1 Solution Stability Tests.....	10
3.2 Buffers .....	10
3.3 Phase Separation.....	13
3.4 Wall Sorption .....	15
3.5 Sorption Kinetics .....	16
3.6 Reversibility .....	16
3.7 Errors and Reproducibility .....	16
4 RESULTS.....	18
4.1 Data Presentation .....	18
4.2 Zn Sorption Data .....	20

4.2.1	Zn Sorption Edges.....	20
4.2.2	Zn Sorption Isotherms .....	21
4.3	Ca Sorption Data.....	25
4.4	Ni Sorption Data .....	27
4.4.1	Ni Sorption Edges as a Function of Ionic Strength .....	27
4.4.2	Ni Sorption Isotherms.....	29
4.5	Isotherms for Ca, Mg, Mn and Zn Deduced from Figures 1a-1d .....	37
5	CATION EXCHANGE .....	39
5.1	Background .....	39
5.2	Selectivity Coefficient Values for Zn, Ca and Ni.....	41
6	CONCLUDING REMARKS .....	44
	ACKNOWLEDGEMENTS .....	47
	REFERENCES .....	48

## LIST OF FIGURES

Fig. 1:	(a) to (g): Aqueous concentrations of Ca, Mg, Mn, Zn, Si, Al and Fe in batch acid/base titration tests after one (O) and seven (●) day equilibration times. The NaClO <sub>4</sub> background electrolyte concentration was 0.5 M. ....	2
Fig. 2:	The solubility of Ni(OH) <sub>2</sub> in 0.1 M NaClO <sub>4</sub> calculated as a function of pH using the thermodynamic data compiled by PEARSON & BERNER (1991). ....	11
Fig. 3:	The solubility of Zn(OH) <sub>2</sub> in 0.1 M NaClO <sub>4</sub> calculated as a function of pH using the thermodynamic data compiled by PEARSON & BERNER (1991). ....	11
Fig. 4:	Ni sorption edges measured in the presence (O) and absence (●) of buffers on conditioned Na-montmorillonite in 0.1 M NaClO <sub>4</sub> . ....	14
Fig. 5:	Zn sorption edge on conditioned Na-montmorillonite in 0.1 M NaClO <sub>4</sub> (▲). Data from Figure 5, Part I (●).....	21
Fig. 6:	Zn sorption isotherm on conditioned Na-montmorillonite in 0.1 M NaClO <sub>4</sub> at pH=5.6. ....	23
Fig. 7:	Zn sorption isotherm on conditioned Na-montmorillonite in 0.1 M NaClO <sub>4</sub> at pH=7.0. ....	24
Fig. 8:	Ca sorption edge on conditioned Na-montmorillonite in 0.1 M NaClO <sub>4</sub> measured after 1 (O), 3 (●), 7 (Δ) and 21 (▲) days. ....	26
Fig. 9:	Ca sorption edge on conditioned Na-montmorillonite measured in 0.1 M (Δ), 0.03 M (●) and 0.01 M (O) M NaClO <sub>4</sub> ..	26
Fig. 10:	Ni sorption edge on conditioned Na-montmorillonite in 0.1 M NaClO <sub>4</sub> in presence (O) or absence (●) of buffers .....	28
Fig. 11:	Ni sorption edge on conditioned Na-montmorillonite in 0.03 M NaClO <sub>4</sub> . ....	28
Fig. 12:	Ni sorption edge on conditioned Na-montmorillonite in 0.01 M NaClO <sub>4</sub> . ....	29
Fig. 13:	Ni sorption isotherm on conditioned Na-montmorillonite in 0.1 M NaClO <sub>4</sub> at pH=8.2. ....	31

Fig. 14:	Ni sorption isotherm on conditioned Na-montmorillonite in 0.1 M NaClO <sub>4</sub> at pH=7.7. ....	32
Fig. 15:	Ni sorption isotherm on conditioned Na-montmorillonite in 0.1 M NaClO <sub>4</sub> at pH=7.0. ....	33
Fig. 16:	Ni sorption isotherm on conditioned Na-montmorillonite in 0.1 M NaClO <sub>4</sub> at pH=5.9. ....	34
Fig. 17:	Ni sorption isotherm on conditioned Na-montmorillonite in 0.1 M NaClO <sub>4</sub> at pH=5.1. ....	35
Fig. 18:	Ni sorption isotherm on conditioned Na-montmorillonite in 0.1 M NaClO <sub>4</sub> at pH=4.7. ....	36
Fig. 19:	(a)-(d): Sorption edges for Ca, Mg, Mn and Zn deduced from aqueous analysis data, Fig.s 1 (a)-(d), using equation 4. ....	38
Fig. 20:	Sorption of Ni at trace concentrations on conditioned Na-montmorillonite as a function of NaClO <sub>4</sub> concentration. The continuous line is a least squares fit with a gradient of -1.9 ....	43
Fig. 21:	Sorption of Ni at trace concentrations on conditioned Na-montmorillonite as a function of NaClO <sub>4</sub> concentration. The continuous line is a least squares fit with a gradient of -2.1 ....	43
Fig. 22:	Diagrammatic representation of Ni sorption on Na-montmorillonite as a function of pH, ionic strength (NaClO <sub>4</sub> concentration), and Ni equilibrium concentration. ——— Contribution of surface complexation to sorption (The max. theoretical value given by the ≡SOH site capacity ) ----- Contribution of cation exchange sorption (The max. theoretical contribution corresponds to the CEC) Note that the overall sorption is given by the sum of the cation exchange and surface complexation contributions for a given set of conditions. Bounding concentrations are : Background Ni concentration and Ni solubility limits. (See text for details.) .....	46

**LIST OF TABLES**

Table 1: Buffers used in the sorption measurements (Data taken from PERRIN & DEMPSEY 1974).....	12
Table 2: Effect of buffer concentration on Ni sorption. ....	13
Table 3: Experimental conditions for the Zn sorption edge measurements on conditioned Na-montmorillonite. ....	20
Table 4: Experimental conditions for the Zn isotherm measurements at pH = 5.6 and 7 on conditioned Na-montmorillonite. ....	21
Table 5: Experimental conditions for the Ca sorption edge measurements on conditioned Na-montmorillonite. ....	25
Table 6: Experimental conditions for the Ni sorption edge measurements on conditioned Na-montmorillonite. ....	27
Table 7: Experimental conditions for the Ni sorption isotherm measurements on conditioned Na-montmorillonite. ....	29
Table 8: Inventories of Ca, Mg, Mn and Zn. ....	37
Table 9: Calculated selectivity coefficients for Ni-Na, Ca-Na and Zn-Na exchange from experimentally measured sorption data. ....	42
Table 10: Selectivity coefficients for Zn-Na, Ni-Na and Ca-Na exchange on montmorillonite. ....	42



## 1 INTRODUCTION

### 1.1 General

The present work covers sorption investigations on conditioned Na-montmorillonite using Ni, Zn and Ca radiotracers under a wide variety of conditions. Sorption edges (log [distribution ratio] versus pH) and sorption isotherms were measured as a function of background electrolyte concentration, pH, solid to liquid (S:L) ratio and radionuclide concentrations/inventories.

The first report (BAEYENS & BRADBURY 1995) dealt with (i) the conditioning ("purifying") procedures applied to the "as received" SWy-1 Na-montmorillonite\*, (ii) the determination of physico-chemical properties and (iii) forward and back batch titration measurements. In particular, the influence of H<sup>+</sup>/cation exchange and background impurities on the form of the titration curves were investigated and discussed. For convenience, we will refer to this work as "Part I" in the rest of this report.

### 1.2 Background

A considerable quantity of data on the compositions of supernatant solutions from batch titration experiments was presented in Part I and enabled us to gain a relatively complete understanding of the fairly complex chemistry of conditioned Na-montmorillonite suspensions at 0.1 and 0.5 M NaClO<sub>4</sub> as a function of pH. The chemical analyses data for Ca, Mg, Mn, Zn, Al, Fe and Si are reproduced here in Figures 1(a) to (g). As shown, the variations in solution chemistry tended to be largest at the extremes of the pH range investigated i.e. pH < 3.5 and pH > 10, and in these regions significant influences on the titration measurements were observed.

---

\* The term "SWy-1 Na-montmorillonite" is used throughout the report to refer to the "as received" Crook County, Wyoming Na-montmorillonite obtained from the Source Clay Minerals Repository, University of Missouri-Columbia, USA.

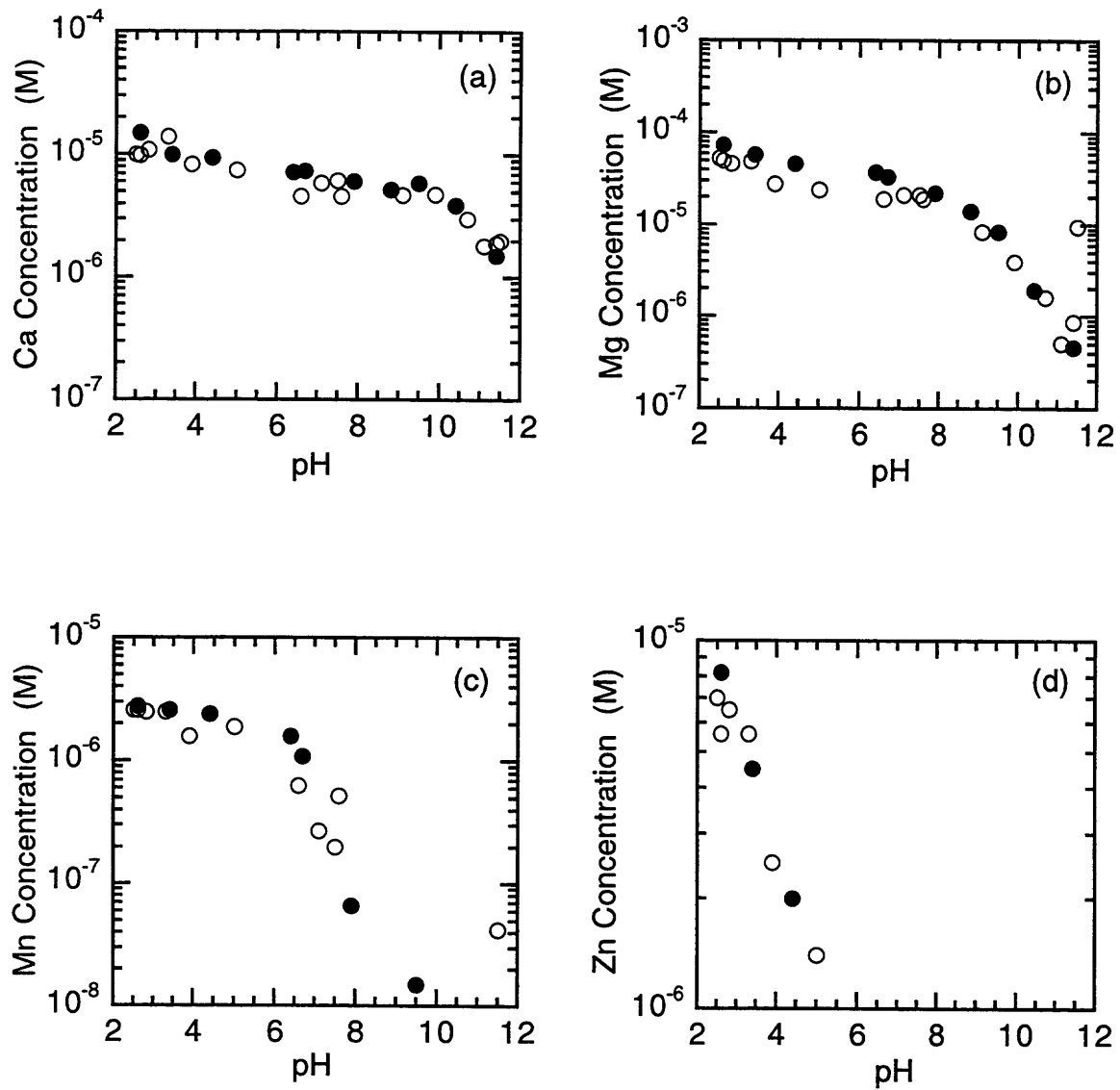


Figure 1: (a) to (d): Aqueous concentrations of Ca, Mg, Mn and Zn in batch acid/base titration tests after one (O) and seven (●) day equilibration times. The  $\text{NaClO}_4$  background electrolyte concentration was 0.5 M.

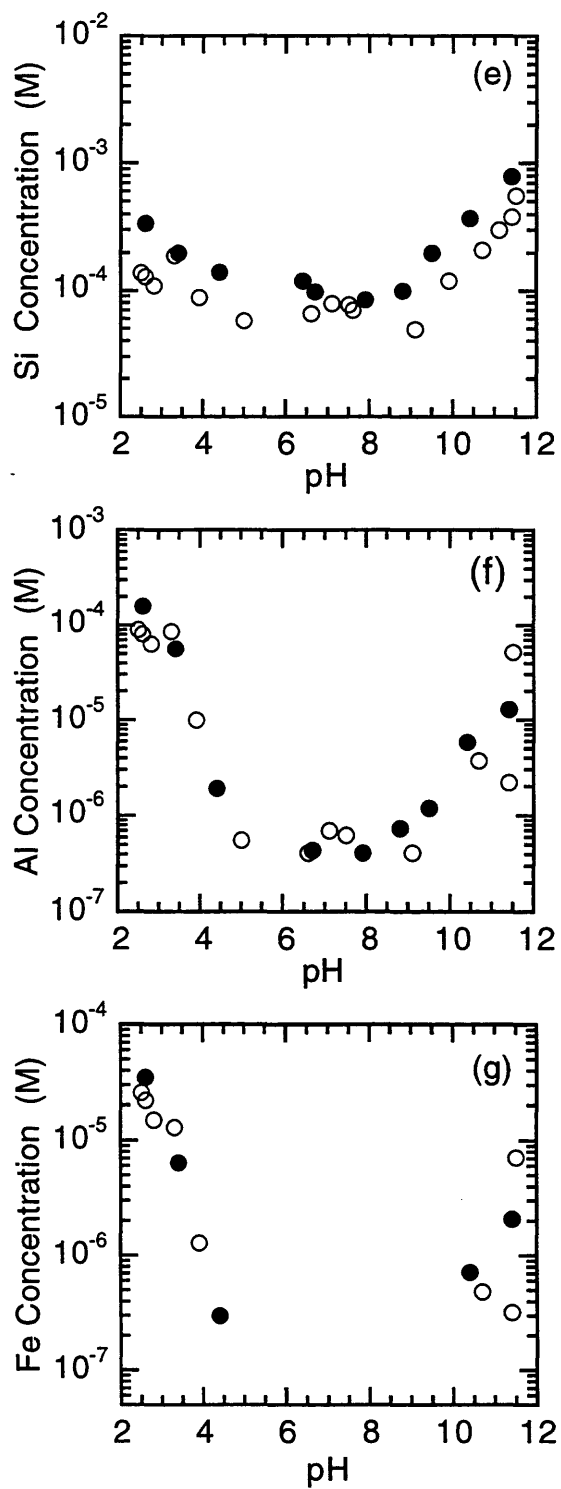


Figure 1: (e) to (g): Aqueous concentrations of Si, Al and Fe in batch acid/base titration tests after one (O) and seven (●) day equilibration times. The  $\text{NaClO}_4$  background electrolyte concentration was 0.5 M.

Background metal impurity concentrations, especially when they vary as a function of experimental conditions, e.g. pH, can have an important influence on radionuclide sorption. This potentially significant competitive effect from background cationic species present in solutions is often not addressed in sorption investigations. The reason is that distribution ratios,  $R_d$  values, or sorption isotherms are generally measured only under a single set of fixed chemical conditions and therefore against a constant background of impurities. However, when the intention is to study sorption mechanisms and to develop concepts, models and codes to describe and predict radionuclide sorption under a wide variety of conditions, then being able to quantify the influences of background impurities may be crucial to a proper understanding of the system.

In the following we will briefly summarise the most important information from Part I which is relevant to the sorption studies presented here.

The main background cations present in solution, and which need to be considered, are the alkaline earth metals Ca and Mg, the transition metals Mn, Zn and Fe, and, in addition Al and Si, see Figure 1. (Analyses for Cu, Cd, Co, Ni and Pb were carried out using ICP-AES but their aqueous concentrations were always below detection limits.)

Ca, Mg and Mn can be considered together since key features of their behaviour are broadly the same. The main sorption mechanism at low pH is cation exchange, and when such reactions are blocked, as here in the high ionic strength background electrolyte, these cations are all predominantly present in solution. As can be seen from Figures 1 (a) to (c), all three exhibit constant concentrations in the low pH region and we interpreted these plateau values as being representative of the inventory of each of these cations in this system. These data, together with some corroborating results obtained from acid extraction experiments, led us to values of  $\sim 10^{-3}$  and  $\sim 4 \times 10^{-4}$  mol kg<sup>-1</sup> for the intrinsic inventories of Ca and Mn respectively. The intrinsic inventory of Mg was estimated to lie between  $3 \times 10^{-3}$  and  $6 \times 10^{-3}$  mol kg<sup>-1</sup>. As the pH increases, a pH dependent sorption component (surface complexation) becomes increasingly important, leading to decreases in the aqueous concentrations. These decreases occur at pH  $\sim 6$  for Mn, pH  $\sim 8$  for Mg, and pH  $\sim 10$  for Ca.

Zn was investigated in somewhat more detail and was concluded to have an intrinsic inventory  $\sim 10^{-3}$  mol kg<sup>-1</sup>. Sorption by surface complexation became dominant at pH  $\sim 3$ .

The general conclusion from these findings was that the sorption characteristics of Ca and Zn should be investigated in more detail. Calcium, because it is almost always present in natural groundwaters, usually at relatively high concentrations ( $\sim 10^{-3}$  M), and Zn because the intrinsic inventory is quite large in comparison with the "strong site" sorption capacity of Namontmorillonite (see BRADBURY & BAEYENS 1995). This, coupled with an apparently strong surface complexation sorption component beginning already at pH  $\sim 3$ , implied that Zn might be an important competitive background cation. In the trace Ni sorption experiments for example (section 5.4.1) the added Ni inventories were significantly less than the intrinsic Zn inventory.

No additional experiments were carried out for Mg and Mn but the aqueous concentration data in Figure 1 (b) and (c) will be considered later and used to derive sorption edges in section 5.5.

The variations of Fe and Al concentrations as a function of pH are both distinctly different from those of Ca, Mg, Mn and Zn, (see Figures 1 (f) and (g)), and were semi-quantitatively interpreted in terms of Fe and Al solid phases. (At extreme pH values, clay mineral dissolution may also be contributing to the concentrations.)

Batch sorption experiments, with very low additions of carrier free <sup>59</sup>Fe (see Figure 6 in Part I), indicated relatively weak and approximately constant "sorption" over the pH range 3 - 7. A proper interpretation of such measurements in the presence of Fe containing solid phases is obviously difficult. However, the important point here is that there was no evidence for a strong pH dependent sorption edge. In view of these results we felt justified in assuming that Fe, at least to a first approximation, is not a significantly competitive cation.

The source of Al in the system may be one or more solid phases and the Na-montmorillonite itself, depending on the pH. At low pH, sorption by cation exchange occurs, but because of the high exchange capacity of Na-montmorillonite, competitive effects are unlikely to be important. As regards its surface complexation behaviour, we were unable to make any sorption measurements as a function of pH in the appropriate concentration range because there is no suitable radiotracer for Al. Although the measured Al concentration profile over the pH range 4 - 10 was relatively flat, Figure 1 (f), this cannot be taken as an indication of constant sorption since Al containing solid phases are present. Solubility effects probably play a role in all Al sorption experiments on montmorillonite, making the interpretation of such measurements very difficult. Because of the lack of reliable and quantitative data on Al sorption at the concentrations and over the pH ranges required, the influence of Al on the measurements remains unclear.

## **2 MATERIALS AND METHODS**

### **2.1 Na-montmorillonite**

Suspensions of conditioned Na-montmorillonite ( $\sim 10$  gram litre<sup>-1</sup>, particle size  $< 0.5$   $\mu\text{m}$ ), were prepared in 0.1 M NaClO<sub>4</sub> solutions from the "as received" SWy-1 material. These suspensions were used throughout this work and the preparation procedures are fully described in Part I.

No further treatment of the conditioned Na-montmorillonite was necessary for experiments carried out in 0.1 M NaClO<sub>4</sub> solutions. In those cases where tests were performed at lower NaClO<sub>4</sub> concentrations, a dialysis method was used to achieve the required background electrolyte concentrations.

### **2.2 Radiotracers**

Acidic source radiotracer solutions of <sup>45</sup>Ca, <sup>63</sup>Ni (both with carrier) and <sup>65</sup>Zn (carrier free) were purchased from Amersham International Plc., in  $\sim 37$  MBq quantities. Each source solution was diluted in  $\sim 50$  ml of de-ionised water to produce a stock solution at pH  $\sim 2$ . Small aliquots (0.1 - 1 ml) of the stock solution were transferred to a glove box where they were further diluted to give standard solutions at the required concentration. Normally, the standard solutions were allowed to stabilise for at least one day in order to allow processes such as container wall sorption to proceed to completion before being used to label the batch tests.

### **2.3 Analytical Methods**

Radionuclide assays were performed using either a Canberra Packard Tri-Carb 2250 CA liquid scintillation analyser or a Packard Minaxi 5530 auto gamma counter.

pH measurements were taken on a WTW Microprocessor 535 pH meter using Orion 8103 combination pH electrodes.

## 2.4 Experimental Procedures

Batch sorption experiments were designed to produce two main types of data sets which are presented as "sorption edges" and "sorption isotherms". In the former, sorption at trace radionuclide concentrations was determined as a function of pH, and in the latter, sorption was measured as a function of concentration at constant pH. For each individual set of test conditions experiments were normally carried out with duplicate or triplicate samples. Generally, the basic experimental procedures used in these two types of experiment were radionuclide independent and are outlined below.

Details specific to a particular set of experiments such as S:L ratio, nuclide concentrations or any deviations from the standard methodology, will be given in the appropriate results section.

The initial activity levels in experiments were roughly optimised via preliminary scoping tests so that after sorption equilibration, good counting statistics could be obtained for one to five ml samples within a reasonable counting time, generally < 30 minutes.

Simultaneously with the preparation of the sorption tests, 10 - 20 aliquots of the standard tracer solutions were transferred to gamma or beta counting vials. These were used as standards whenever any samples from the batch tests were counted. (In the case of  $\beta$ -active standards, the Instagel™ was only added just before counting.)

All experiments were carried out in controlled N<sub>2</sub> atmosphere glove boxes: CO<sub>2</sub> ~ 5 ppm, O<sub>2</sub> ~ 5 ppm.

### 2.4.1 Sorption Edge Determinations

Sorption edge measurements were always carried out at trace radionuclide concentrations. "Trace" in this context means the lowest possible initial concentrations in the batch tests compatible with good counting statistics after sorption. (Indications of the actual concentrations of tracer added for each radionuclide investigated are given later.)

Generally, 5 ml aliquots of conditioned Na-montmorillonite suspensions (corresponding to ~ 50 mg Na-Montmorillonite) were pipetted from the vigorously stirred stock suspension into 50 ml polypropylene centrifuge tubes. An appropriate volume of buffer solution (see section 3.2) at the required pH was added to each reaction vessel (20 ml) so that when all the components for the experiment were together, the buffer concentration was  $10^{-3}$  M (see section 4.2). In cases where no buffers were used, the pH was set with additions of either NaOH or HNO<sub>3</sub> Titrisol™ solutions. As the last step in the preparation procedure, the standard tracer solution, at the appropriate concentration of NaClO<sub>4</sub>, was added (10 ml). The centrifuge tubes were then closed with screw caps and shaken end-over-end for at least two days (see section 4.5). Subsequently they were removed from the glove box and centrifuged at 95,000g (max.) for one hour before returning them to the glove box for pH measurement and sampling of the supernatant solution. Duplicate samples, together with the standards, were counted for times long enough to give a one sigma (or better) error in the determinations. For  $\beta$ -active radionuclides the ratio of Instagel™ to sample solution was 3:1.

#### **2.4.2 Isotherm Determinations**

A series of salt solutions covering the nuclide concentration range required was made up at the desired pH in constant NaClO<sub>4</sub> background electrolyte concentrations (mainly 0.1 M) containing  $10^{-3}$  M buffer. These solutions were then labelled at the appropriate level with the corresponding radionuclide from a previously prepared standard tracer solution.

Volumes of conditioned Na-montmorillonite suspensions similar to those indicated in section 3.4.1 were pipetted into 50 ml centrifuge tubes and the labelled salt solutions added, (30 ml). The procedure from this point on was the same as that already described above.

In the following chapter we will address certain key operations in the experimental methodology which are critical to the accuracy and reproducibility of the measurements.

### 3 EXPERIMENTAL TECHNIQUES

#### 3.1 Solution Stability Tests

Solubility calculations for Ni and Zn, shown in Figures 2 and 3 respectively, were used to estimate the experimental pH/concentration conditions for which solutions of each nuclide should be stable. The graphs show very steep decreases in solubilities with increasing pH. Since thermodynamic data cannot always be relied upon, the stabilities of Ni and Zn solutions used in the sorption isotherm measurements were checked prior to performing the experiments.

The activities of  $^{63}\text{Ni}$  labelled solutions of  $\text{Ni}(\text{NO}_3)_2$ , having concentrations between  $5 \times 10^{-8}$  and  $10^{-4}$  M, were measured in the pH range 7 - 10 at 2, 6 and 40 day intervals. Below pH 8 all Ni solutions in the concentration range investigated were stable and exhibited little or no wall sorption. (The highest initial concentration of  $\text{Ni}(\text{NO}_3)_2$  used in the sorption isotherm experiments was  $5 \times 10^{-5}$  M at pH = 8.2.) Between pH 8 and 8.5 up to 15% of the Ni inventories were lost to wall sorption at all concentrations, otherwise the solutions were stable. Further losses in activities after centrifugation (95,000g max., 1 hour) were observed for pH values > 8.5. The solubilities of Ni were largely as expected from the calculated values given in Figure 2.

In the case of Zn, the highest starting concentration used was  $5 \times 10^{-4}$  M at pH=7. This is ~ 10 times lower than the calculated solubility limit of ZnO, see Figure 3.

#### 3.2 Buffers

In the early series of sorption edge experiments, the pH in each batch test was set individually to the required value using additions of Titrisol™  $\text{HNO}_3$  or NaOH. It soon became apparent that in the pH range ~ 5 to ~ 9 there was often an unacceptably large scatter in the data, reproducibility was poor and the results were, to some extent, time dependent. (At set pH values outside the above range such difficulties were not encountered.) Since for many nuclides the sorption edges occur predominantly between pH 5 and 9, the scatter and poor reproducibility in the measurements meant that it was very difficult to define a reliable sorption edge.

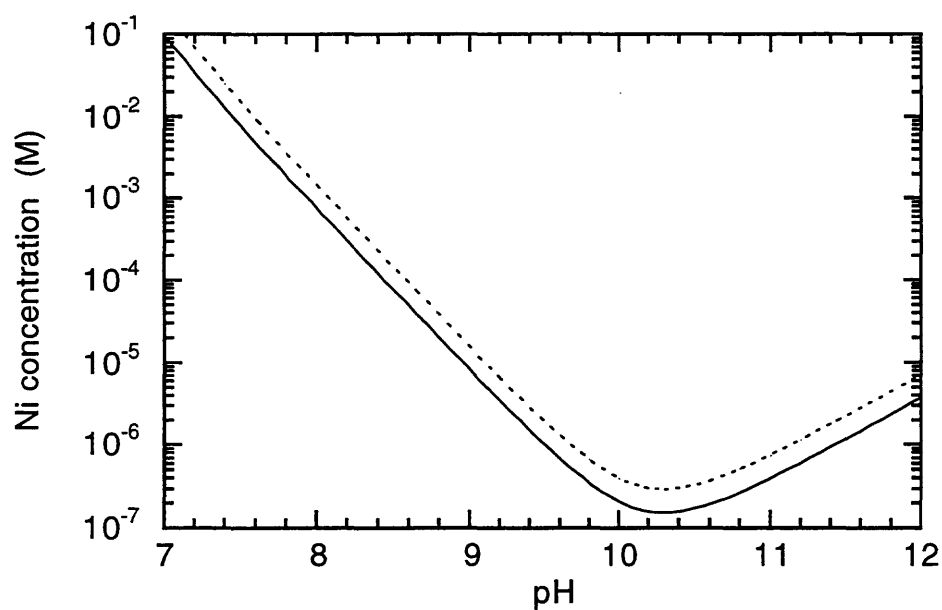


Figure 2: The solubility of  $\text{Ni(OH)}_2$  (dotted line) and  $\text{NiO}$  (continuous line) in 0.1 M  $\text{NaClO}_4$  calculated as a function of pH using the thermodynamic data compiled by PEARSON et al. (1992).

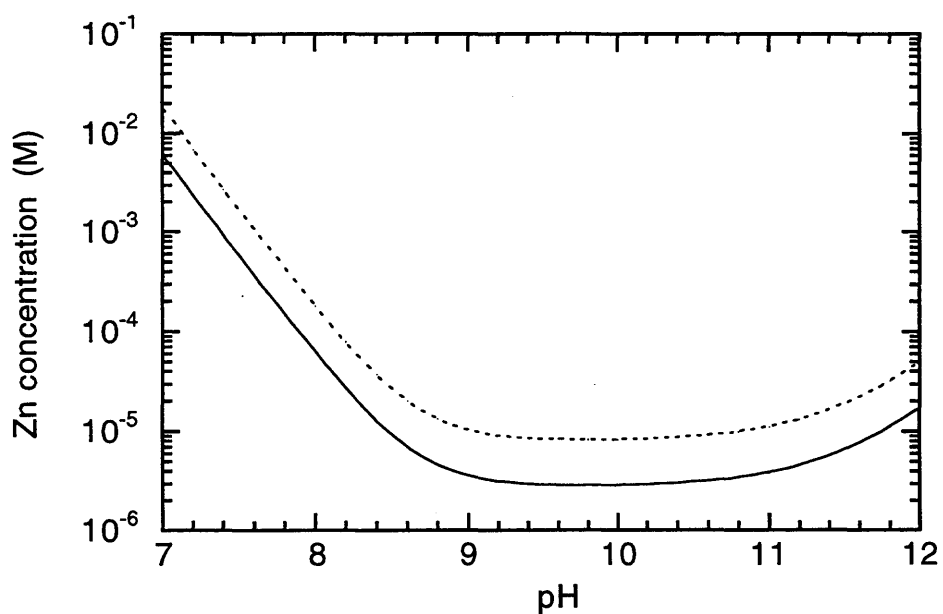


Figure 3: The solubility of  $\text{Zn(OH)}_2$  (dotted line) and  $\text{ZnO}$  (continuous line) in 0.1 M  $\text{NaClO}_4$  calculated as a function of pH using the thermodynamic data compiled by PEARSON et al. (1992).

The main cause of the problem was traced to the pH measurements. First, pH values set anywhere in the range between 5 and 9 tended to drift up or down towards neutral pH. (This effect had also been noticed in the batch titration experiments reported in Part I) Secondly, separate experiments showed that the time for the pH electrode to reach a steady state value in the pH range ~ 5 to ~ 8 could be as long as 1 hour. (Such long equilibration times would present practical difficulties since a normal experiment consisted of 30 or more individual tests.) These two factors led to uncertainties in pH measurements which were estimated to be as much as  $\pm 0.5$  units.

As a consequence of the above, it was decided to test whether buffers could be used in batch sorption experiments to fix the pH at set values without influencing the sorption. The buffers given in Table 1 were chosen because of their very weak complexation with metals (PERRIN & DEMPSEY 1974).

The buffers were tested in two ways. First, trace Ni sorption on conditioned Namontmorillonite in 0.1 M NaClO<sub>4</sub> solutions at an S:L ratio of 1.5 gram litre<sup>-1</sup> was measured in the presence of buffer solutions ranging in concentration from  $2 \times 10^{-4}$  to  $2 \times 10^{-2}$  M. The results are given in Table 2 and as can be seen the influence of buffer concentration on the magnitude of sorption in the range measured is insignificant. On the basis of these results we chose to standardise the buffer additions in sorption experiments at  $10^{-3}$  M.

Table 1: Buffers used in the sorption measurements (Data taken from PERRIN & DEMPSEY 1974)

Buffer	pK <sub>a</sub>	pH range
AA (acetic acid)	4.76	4.3 - 5.3
MES (2-(N-Morpholino)ethane-sulphonic acid)	6.15*	5.7 - 6.7
MOPS (3-(N-Morpholino) propanesulphonic acid)	7.20	6.8 - 7.7
TRIS (Tris(hydroxymethyl)aminomethane)	8.06	7.5 - 8.5
CHES (3-(cyclohexyl amino)ethanesulphonic acid)	9.55*	9.0 - 10.0

\* Conditional constant for 0.1 M solution.

In a second series of experiments a sorption edge for Ni at trace concentrations was extracted from a large number of measurements carried out in the pH

range 4 - 9 without using buffers. A repeat set of tests in the presence of  $10^{-3}$  M buffer was performed under similar conditions. The results, given in Figure 4, demonstrate clearly that these buffers do not influence the sorption behaviour to any significant extent.

Table 2: Effect of buffer concentration on Ni sorption

Buffer	Buffer concentration (M)	log $R_d$ (litre $kg^{-1}$ )	pH
MES	$2 \times 10^{-2}$	2.8	6.3
	$2 \times 10^{-3}$	2.9	6.4
	$2 \times 10^{-4}$	3.0	6.7
MOPS	$2 \times 10^{-2}$	3.5	7.4
	$2 \times 10^{-3}$	3.4	7.4
	$2 \times 10^{-4}$	3.3	7.3
TRIS	$2 \times 10^{-2}$	3.6	8.2
	$2 \times 10^{-3}$	3.9	8.1
	$2 \times 10^{-4}$	3.6	7.7
CHES	$2 \times 10^{-2}$	4.3	9.6
	$2 \times 10^{-3}$	4.3	9.5

Finally, the buffers used are organic ligands, and as such, could cause variable quenching effects when present in samples being counted on a liquid scintillation counter. This possibility was thoroughly checked and no adverse effects on the counting due to any of the buffers was detected.

### 3.3 Phase Separation

Throughout this work phase separations were carried out by centrifugation in a Beckman L7 Ultracentrifuge. 50 ml polyethylene centrifuge tubes or 250 ml bottles were used as reaction vessels and the standard procedure was to centrifuge for one hour at 95,000 g max. or 39,000 g max., respectively. The only disadvantage of this procedure was that samples had to be removed from the glove box for centrifugation and then returned for sampling.

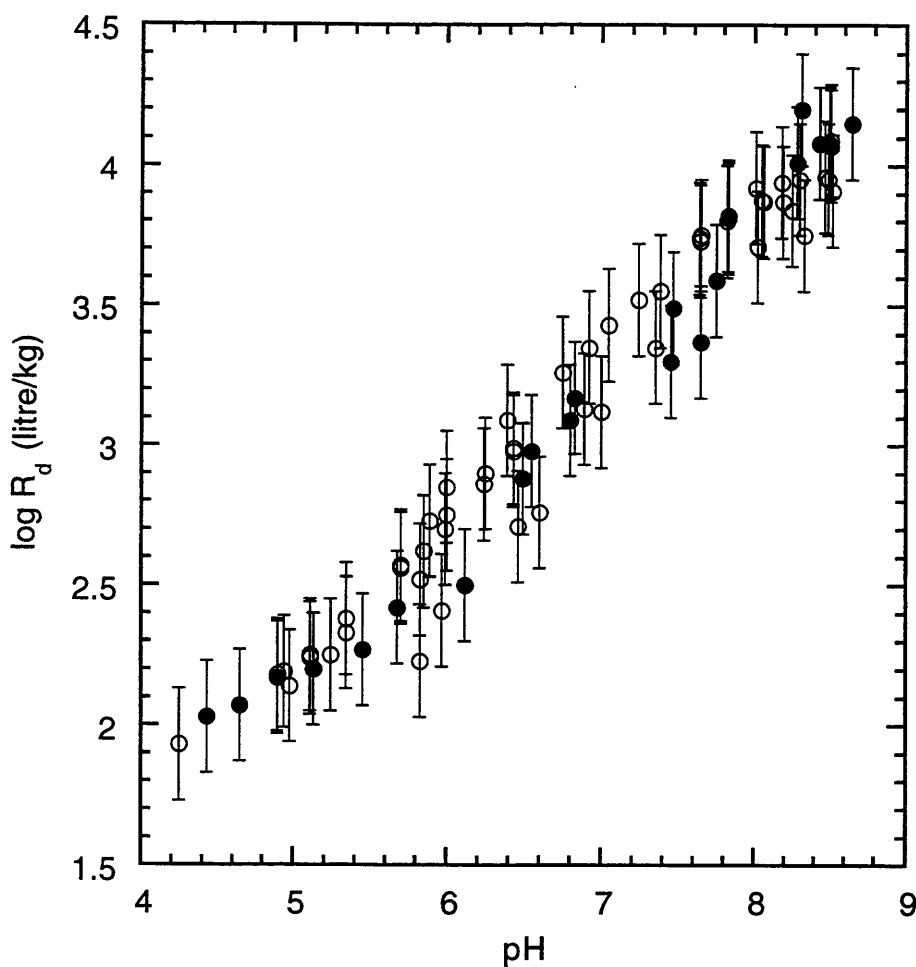


Figure 4: Ni sorption edges measured in the presence (O) and absence (●) of buffers on conditioned Na-montmorillonite in 0.1 M NaClO<sub>4</sub>

Estimates made using Stoke's Law indicated that centrifuging at 95,000 g max. under the geometrical conditions appropriate to a Type 28 fixed angle rotor was sufficient to sediment all colloidal particles > 10 nm in ~ 20 minutes.

A study described in Part I compared the phase separation efficiency of centrifugation with solid material containment in dialysis bags (pore size ~ 2.5 nm) over a range of pH values. No significant differences between the two methods were found.

In some batch sorption tests 250 ml centrifuge bottles were used as reaction vessels, and these could only be centrifuged at 39,000g max. In order to check

whether this had any significant influence on the measurements, the following tests were performed. Trace Ni sorption experiments with Na-montmorillonite suspensions were performed in 250 ml bottles and allowed to reach equilibrium. Forty ml aliquots from the strongly stirred suspension were then transferred to 50 ml centrifuge tubes, shaken for 1 day and the contents discarded. (This procedure conditioned the tube walls to the activity levels in the suspensions.) A further 40 ml of suspension was then transferred to each 50 ml tube, followed by the standard centrifugation, sampling and counting procedures. The 250 bottles were also sampled after centrifugation, but at 39,000 g max. The spread in each set of ten measurements from each tube or bottle was greater than the differences between the averaged values for the 50 and 250 ml vessels.

### **3.4 Wall Sorption**

Wall sorption is unavoidable in batch sorption tests. We considered that the normal method of measuring wall sorption in blank experiments, and using these data to calculate errors in the sorption measurements yielded error values which were too pessimistic. (Competitive sorption effects between the solid phase and the wall are ignored.)

Instead, we decided to measure wall sorption directly as a function of pH. A series of samples were selected from Ni sorption edge and isotherm experiments (see Chapter 4) after they had been completed. The contents of each bottle were poured away, the bottles rapidly rinsed once with de-ionised water and then the internal surfaces lightly wiped to remove any remaining fluid. Twenty ml of 0.1 M HNO<sub>3</sub> were added and acid leaching allowed to occur for 4 days on an end-over-end shaker. The counting results indicated that the extent of wall sorption depended on the pH in the original experiment. The quantities taken up by the wall surfaces increased from ~ 0.1 to 0.5% of the initial activity over the pH range ~ 4.5 to ~ 8.2. (In separate tests, carried out in the absence of Na-montmorillonite but otherwise under similar conditions, wall sorption accounted for more than 30% of the initial activity at pH ~ 8.) For the conditions used in the majority of experiments described in this report, the effect of wall sorption is to introduce an uncertainty in the log R<sub>d</sub> values of ~ 0.05 log units.

### **3.5 Sorption Kinetics**

Sorption kinetic measurements were carried out for all the radionuclides investigated. In general the kinetic tests were performed at trace concentrations in buffered 0.1 M NaClO<sub>4</sub> suspensions of conditioned Na-montmorillonite (S:L ratio of 1.5 gram litre<sup>-1</sup>) as a function of pH for times between 1 and 18 days. No kinetic effects were observed i.e. after 1 day end-over-end shaking the uptake of radionuclides was complete. Batch sorption experiments were always shaken for at least 2 days and sometimes as long as 7 days. (Times longer than 2 days were chosen purely for reasons of practical convenience.)

### **3.6 Reversibility**

A critical point which is not directly addressed here is sorption reversibility. Reversibility is an important condition for applying mass action relationships to describe sorption. We would like to state that we have studied reversibility and that the "reversibility criterion" is fulfilled, at least in the range of pH values for which sorption data are presented. However, the situation is relatively complex and very different kinetics govern the sorption and desorption processes. We did not want to detract from the main theme of the work described in this report by engaging in a long discussion of the methodology and results obtained in the reversibility experiments. Instead we decided to cover this topic separately, and it will form part of a future paper.

### **3.7 Errors and Reproducibility**

A formal estimate of the maximum absolute error calculated by considering the maximum error in each operation in a batch sorption experiment yielded, in the worst case, an uncertainty in log R<sub>d</sub> of ~0.15 log units. ("Worst case" here means the error associated with measurements made under the most unfavourable conditions used in any sorption test i.e. a low sorption value determined at a very low S:L ratio.)

Over a period of approximately 18 months the sorption edge for Ni at trace concentrations was, for various reasons, measured on five separate occasions, see Figure 10. Different batches of conditioned Na-montmorillonite at different

S:L ratios were used in these tests and the co-workers making the measurements were different. Also, although the Ni concentrations were always at trace levels, the actual Ni inventories varied slightly. Such a series of measurements provided a good indication of the overall reproducibility of the experimental data. An uncertainty in the  $\log R_d$  values of  $\pm 0.2$  log units covered the spread of the measurements over the whole pH range in Figure 10. This value has been taken as a realistic uncertainty level in sorption measurements covering all possible sources of error and has been applied generally to all sorption measurements presented in the subsequent chapters.

## 4 RESULTS

The main purpose of this chapter is to present the sorption edge and isotherm data measured for Ni, Zn and Ca in the Na-montmorillonite system. The aim here is not to discuss these data in detail, but rather to restrict ourselves to a few comments which are either relevant to the experimental techniques or which aid, in a general way, an understanding of the data. Detailed discussions and quantitative interpretations of the sorption behaviour will be given in the report on the modelling work (BRADBURY & BAEYENS 1995).

### 4.1 Data Presentation

Sorption edges are most commonly given as a plots of the percentage, or fraction, of the radionuclide inventory sorbed versus pH. In the work described here we have chosen to present such data in terms of the logarithm of the distribution ratio,  $R_d$ , plotted against pH. If  $R_d$  is defined in the customary manner as

$$R_d = \frac{C_{init.} - C_{eq.}}{C_{eq.}} \cdot \frac{V}{m} \quad [1]$$

where:  $C_{init.}$ : initial aqueous concentration of active and inactive metal  
 $C_{eq.}$ : equilibrium aqueous concentration of active and inactive metal  
 V: volume of liquid phase (litre)  
 m: mass of solid phase (kg)

then the relation between the fraction of the radionuclide sorbed,  $F$ , and  $R_d$  is:

$$F = \frac{R_d}{R_d + \frac{V}{m}} \quad [2]$$

For practical reasons we used S:L ratios throughout this work of ~ 1 gram of conditioned Na-montmorillonite per litre. When results are expressed as "% sorbed", it can readily be shown that for the S:L ratio quoted above, the higher sorption values are concentrated in the last tenth of the scale i.e. between ~ 90 and ~ 100% sorbed. However, when plotted on a log  $R_d$  scale the same data extend over 2 orders of magnitude. Fitting/modelling data presented in the latter form is much more sensitive to the choice of parameters (BRADBURY &

BAEYENS 1995). Fits which may appear visually good on a % sorbed versus pH plot often look poor on a log  $R_d$  versus pH representation.

We would also add that in radioactive waste management and environmental sciences, where the migration of radionuclides/contaminants is of central interest, the quantity of critical importance is the concentration of radionuclide/contaminant in the groundwater along the flow path. We believe that representing sorption data in terms of distribution ratios rather than as "% sorbed" better reflects the sensitivity of the aqueous concentrations to changing conditions.

Sorption isotherm data are presented in two forms; as log [moles of metal sorbed per kg solid] versus log [equilibrium aqueous metal concentration] and as log  $R_d$  versus log [equilibrium aqueous metal concentration]. The former is the more usual presentation (Freundlich type plot) while the latter is more convenient since it allows the variation in distribution ratio as a function of concentration to be seen at a glance.

Zn and Ca were investigated separately as important background cations, see Chapter 1. As will be discussed in the modelling report (BRADBURY & BAEYENS 1995), the minimum sorption data requirements to deduce intrinsic surface complexation constants on two types of sites are a sorption edge at trace concentration, and an isotherm at a fixed pH chosen so that sorption due to surface complexation can be measured over the widest possible concentration range. These data are presented for Zn together with a second sorption isotherm which provided an independent data set for modelling.

Ca, and probably other alkaline earth metals such as Mg, Sr and Ba, is a somewhat special case in that sorption edges measured at trace concentration as function of ionic strength are all that is required to define and model the sorption behaviour. This is discussed further in section 4.3.

The main investigations were centred on Ni. Sorption edges were measured at trace concentrations as a function of  $\text{NaClO}_4$  background electrolyte concentration. Sorption isotherms for Ni were determined over a wide range of concentrations at several pH values.

Additional sorption edge data for Ca, Mg, Mn and Zn were deduced from chemical analyses of the supernatant solutions in the batch titration measurements which are reproduced here in Figure 1(a)-(d). The method used for extracting sorption edges from these data is described in section 5.5.

In the following, each set of measurements is accompanied by a summary of the experimental conditions.

## 4.2 Zn Sorption Data

### 4.2.1 Zn Sorption Edges

A sorption edge was measured on conditioned Na-montmorillonite at 0.1 M NaClO<sub>4</sub> using carrier free <sup>65</sup>Zn. The activity levels of <sup>65</sup>Zn used in these experiments corresponded to an added Zn concentration of < 10<sup>-9</sup> M. The results are presented in Figure 5 and the experimental conditions summarised in Table 3.

Table 3: Experimental conditions for the Zn sorption edge measurements on conditioned Na-montmorillonite at 0.1 M NaClO<sub>4</sub>.

Experimental Conditions	Fig. 5 in Part I	Fig.5
pH range	2 - 9.5	3 - 9
Buffers	no	yes
S:L ratio (gram litre <sup>-1</sup> )	1.32	1.16
Intrinsic Zn inventory (mol kg <sup>-1</sup> )	10 <sup>-3</sup>	10 <sup>-3</sup>
Equilibration time (days)	1	7
Number of measurements	15	41

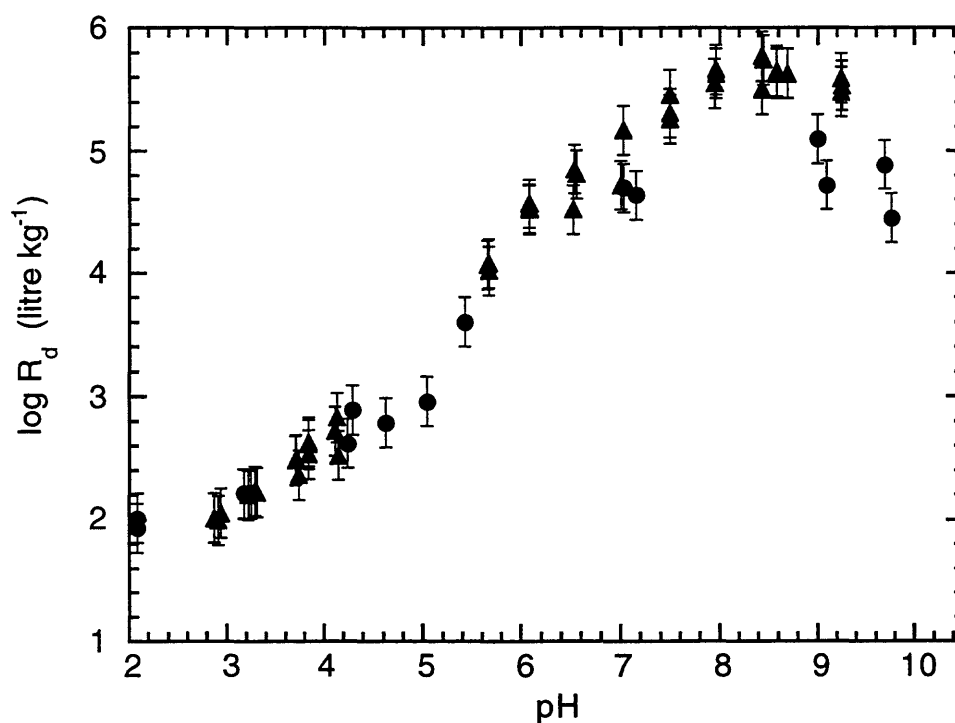


Figure 5: Zn sorption edge on conditioned Na-montmorillonite in 0.1 M NaClO<sub>4</sub> (▲). Data from Figure 5, Part I (●)

#### 4.2.2 Zn Sorption Isotherms

Two sorption isotherms were measured for Zn using carrier free <sup>65</sup>Zn at pH = 5.6 and 7 under the conditions given in Table 4. The results are shown in Figures 6 and 7.

Table 4: Experimental conditions for the Zn isotherm measurements at pH = 5.6 and 7 on conditioned Na-montmorillonite at 0.1 M NaClO<sub>4</sub>.

Experimental Conditions	Fig. 6	Fig. 7
pH	5.6	7
Buffer	MES	MOPS
S:L ratio (gram litre <sup>-1</sup> )	1.16	0.325
Intrinsic Zn inventory (mol kg <sup>-1</sup> )	10 <sup>-3</sup>	10 <sup>-3</sup>
Equilibration time (days)	7	12
Number of measurements	21	25

It was shown in Part I that there is an intrinsic Zn inventory of  $\sim 10^{-3}$  mol kg<sup>-1</sup> associated with the conditioned Na-montmorillonite. One consequence of this is that equilibrium concentrations in sorption tests cannot always be calculated in the normal manner from equation 1 using initial concentrations and  $R_d$  values obtained from activity measurements. Rather, they must be determined from a mass balance equation of the form,

$$V \cdot C_{add.} + m \cdot I_{Zn} = m \cdot R_d \cdot C_{eq.} + V \cdot C_{eq.} \quad [3]$$

where:

$R_d$  = distribution ratio calculated from activity measurements (litre kg<sup>-1</sup>),

$C_{add.}$  = concentration resulting from the addition of inactive ZnCl<sub>2</sub> and active <sup>65</sup>Zn tracer,

$m$  = mass of Na-montmorillonite (kg),

$V$  = volume (litre),

$I_{Zn}$  = intrinsic Zn inventory (10<sup>-3</sup> mol kg<sup>-1</sup>),

$C_{eq.}$  = equilibrium concentration (M).

The intrinsic Zn inventory is unimportant at high Zn concentrations where  $V \cdot C_{add.} \gg m \cdot I_{Zn}$ , but becomes increasingly important as the concentration decreases. For experiments carried out at trace Zn concentration levels (i.e. only active <sup>65</sup>Zn added), the term " $m \cdot I_{Zn}$ " in equation 3 dominates. Also, for a fixed pH and S:L ratio in a system where no Zn salts are added, the background equilibrium concentration of Zn will be fixed by the intrinsic inventory. This Zn concentration represents the lowest equilibrium concentration at which sorption can be measured.

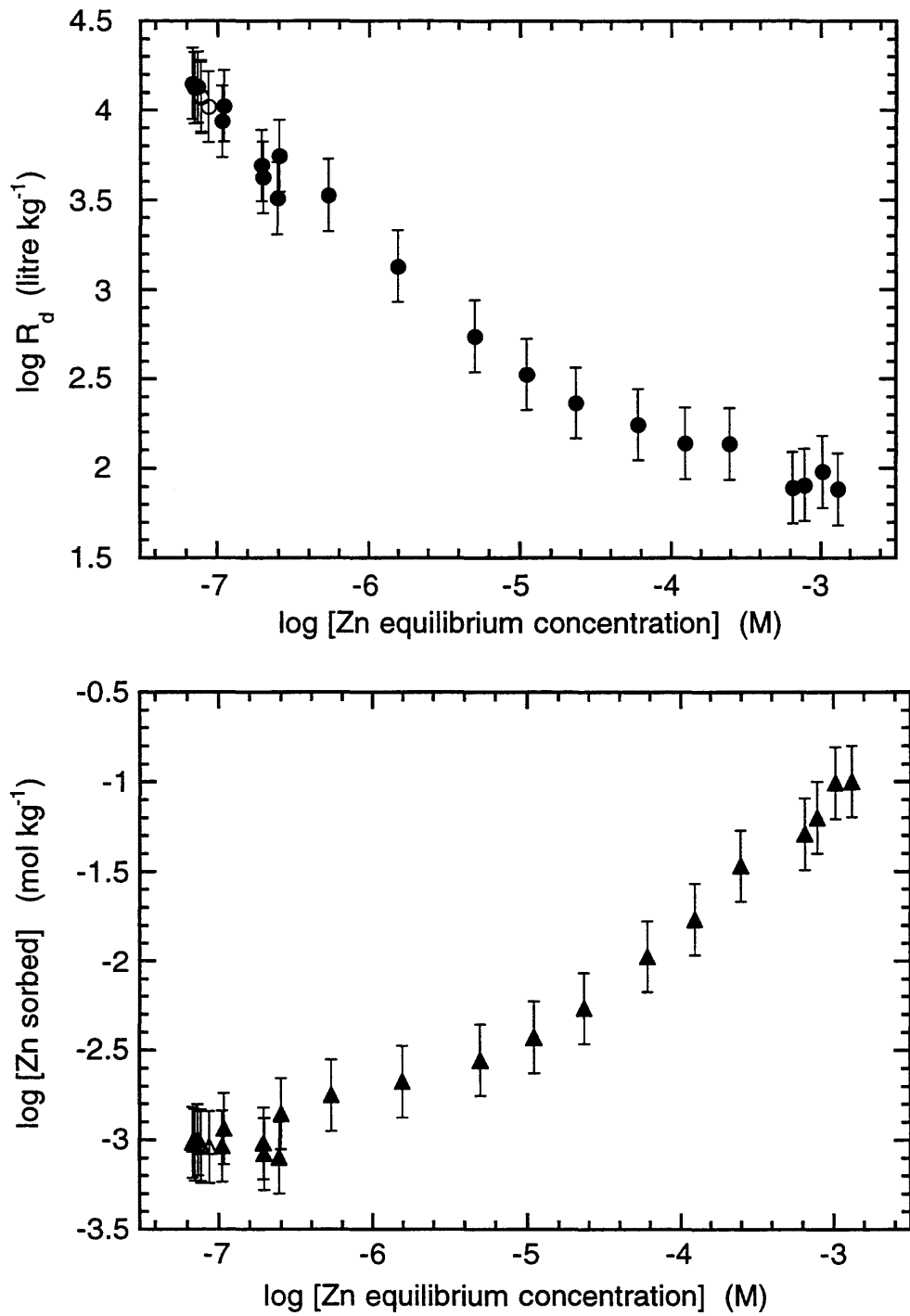


Figure 6: Zn sorption isotherm data on conditioned Na-montmorillonite at pH = 5.6. (Open symbols are data taken from Figure 5)

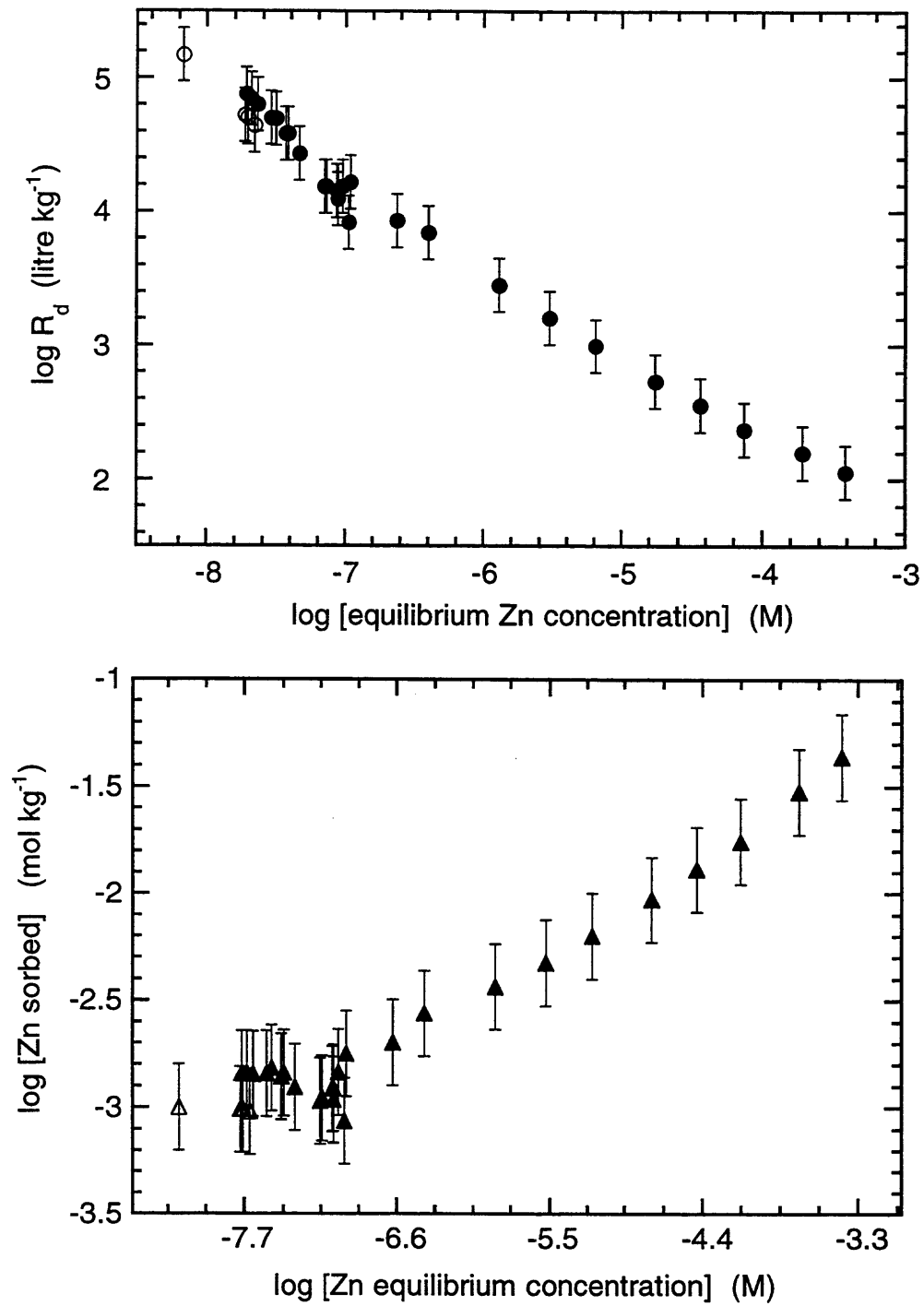


Figure 7: Zn sorption isotherm data on conditioned Na-montmorillonite at pH = 7.0. (Open symbols are data taken from Figure 5)

### 4.3 Ca Sorption Data

Figure 8 shows Ca sorption edges measured at 8 different pH values after equilibration time intervals of 1, 3, 7 and 21 days. (The experimental conditions are given in Table 5.) As can be seen, there are no significant kinetic effects. Ca sorbs predominantly by cation exchange and only at pH values > 8 is there an indication that surface complexation is beginning to contribute to the overall sorption. The above tests were repeated as a function of NaClO<sub>4</sub> concentrations to give sorption edges at 0.03 and 0.01 M, Figure 9. The Ca concentration added to the system by labelling with <sup>45</sup>Ca was ~ 10<sup>-7</sup> M.

Table 5: Experimental conditions for the Ca sorption edge measurements on conditioned Na-montmorillonite.

Experimental Conditions	Edges Figure 8	Edges Figure 9	Single R <sub>d</sub> meas.
NaClO <sub>4</sub> concentration (M)	0.1	0.01; 0.03; 0.1	0.267
pH	5 - 9.5	5 - 9.5	7
Buffers	yes	yes	MOPS
S:L ratio (gram litre <sup>-1</sup> )	1.14	1.14	1.72
Intrinsic Ca inventory (mol kg <sup>-1</sup> )	10 <sup>-3</sup>	10 <sup>-3</sup>	10 <sup>-3</sup>
Equilibration time (days)	1; 3; 7; 21	3	3
Number of measurements	32	16	3

Sorption isotherms were not measured for Ca. Increasing the inventory of any sorbent has the effect of shifting the surface complexation contribution in a sorption edge to higher pH values (see for example DZOMBAK & MOREL, 1990). If we consider Figure 8, the surface complexation component is weak and even at trace Ca concentrations only becomes significant at pH values greater than 8. Increasing the Ca inventory, as in an isotherm experiment, would tend to shift the sorption edge to even higher pH values. Hence, Ca sorption as a function of concentration at any pH up to ~ 10 would be dominated by cation exchange, implying constant sorption. Thus isotherm measurements would not yield any additional useful information.

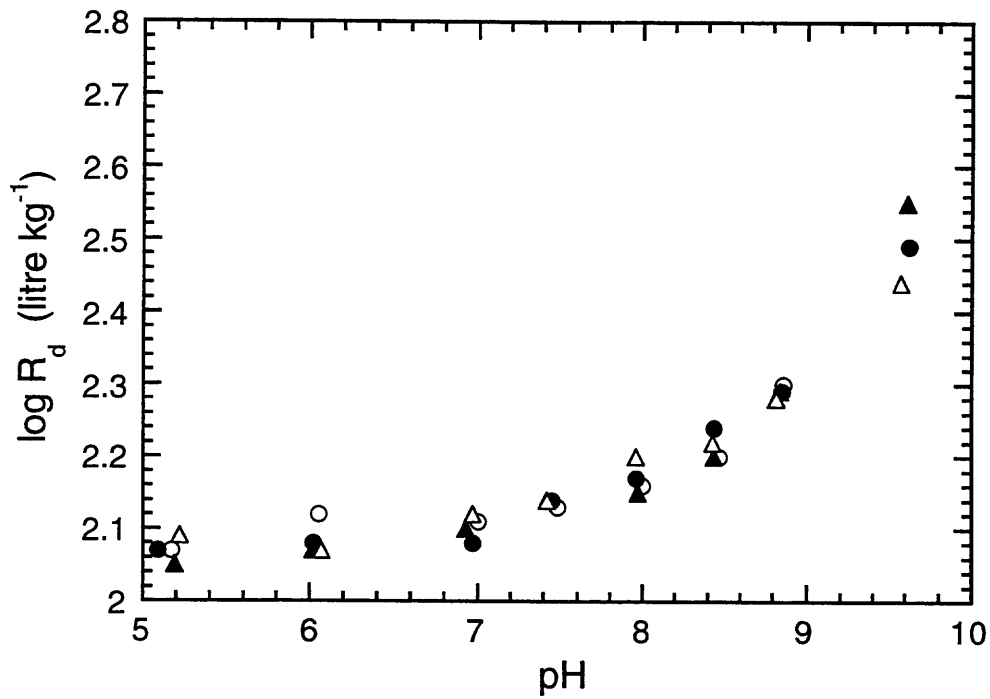


Figure 8: Ca sorption edges on conditioned Na-montmorillonite in 0.1 M NaClO<sub>4</sub> measured after 1 (O), 3 (●), 7 (Δ) and 21 (▲) days

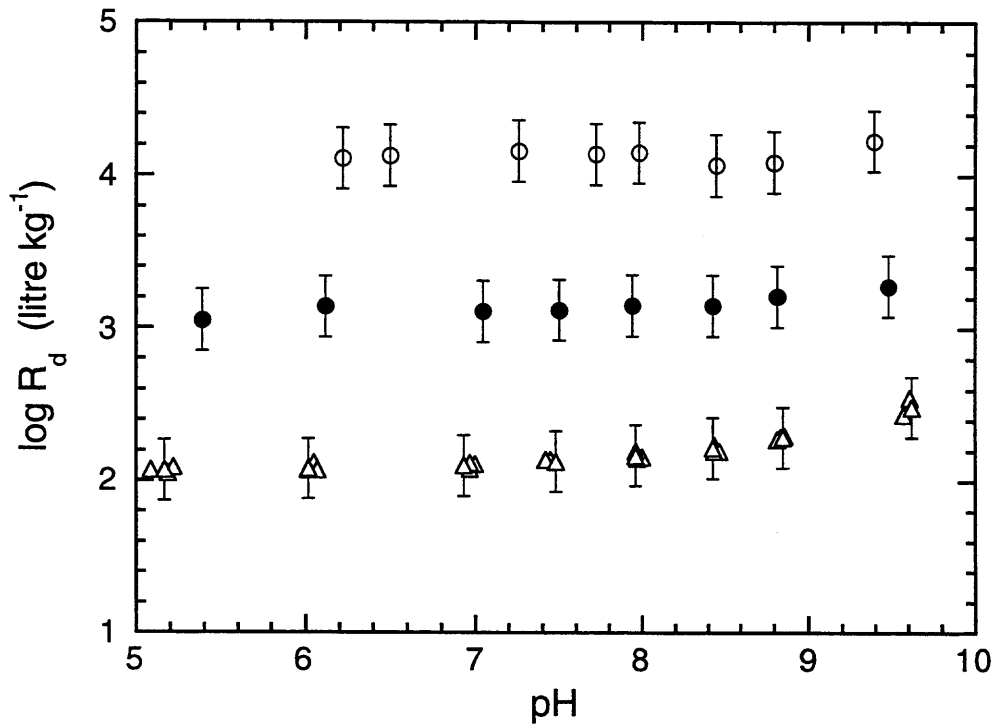


Figure 9: Ca sorption edge on conditioned Na-montmorillonite measured in 0.1 M (Δ), 0.03 M (●) and 0.01 M (O) NaClO<sub>4</sub>

## 4.4 Ni Sorption Data

### 4.4.1 Ni Sorption Edges as a Function of Ionic Strength

Trace Ni sorption edges were determined on conditioned Na-montmorillonite at 3 different NaClO<sub>4</sub> concentrations. The data are presented in Figures 10 - 12 and the corresponding experimental conditions are summarised in Table 6. The Ni concentration added to the system by labelling with <sup>63</sup>Ni was  $< 3 \times 10^{-7}$  M. (Note that in contrast to Zn, Ni was not detected in the Na-montmorillonite, see Table 5, Part I.)

Table 6: Experimental conditions for the Ni sorption edge measurements on conditioned Na-montmorillonite

Experimental Conditions	Fig. 10	Fig. 11	Fig. 12	Single R <sub>d</sub> measurements
NaClO <sub>4</sub> (M)	0.1	0.03	0.01	0.003
pH range	3 - 10	4.5 - 10	4.5 - 10	4-7
Buffers	yes	yes	yes	yes
S:L ratio (gram litre <sup>-1</sup> )	1 - 1.8	1.1	1.1	0.5; 1.1
Equilibration time (days)	1; 7;11;18	4	4	1; 4
Nr. of measurements	90	24	24	14

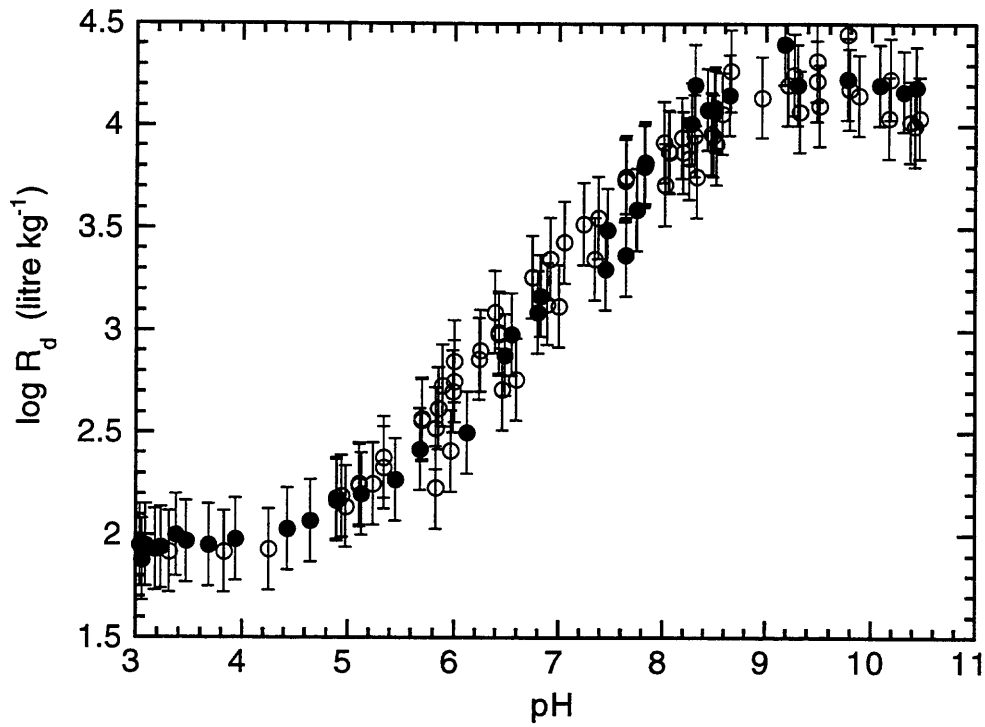


Figure 10: Ni sorption edge on conditioned Na-montmorillonite in 0.1 M  $\text{NaClO}_4$  in presence (O) or absence (●) of buffers

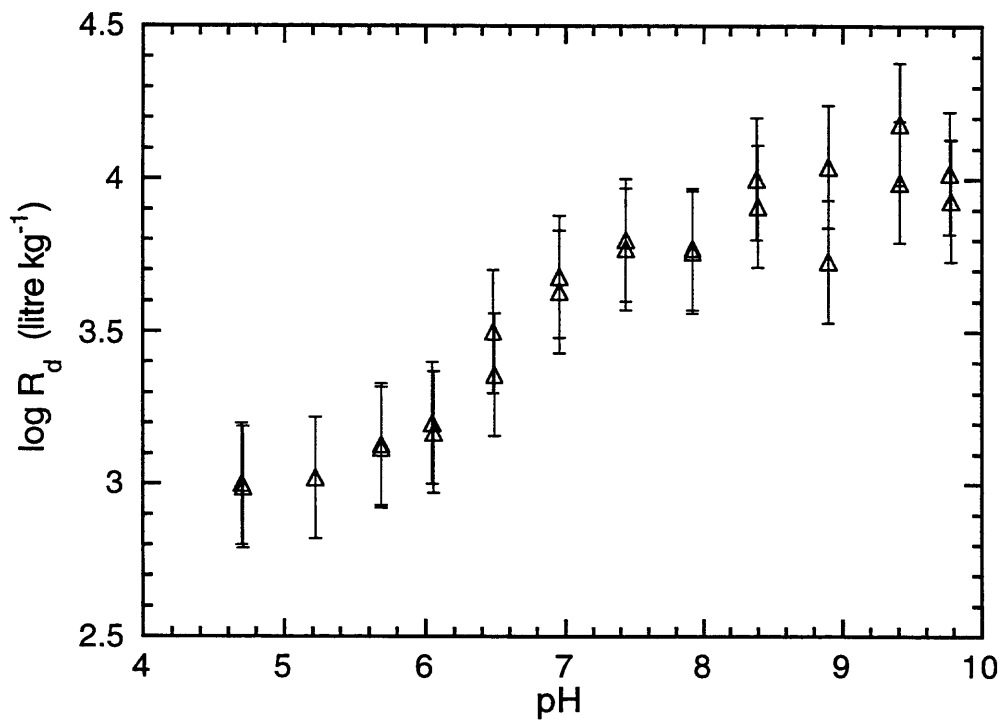


Figure 11: Ni sorption edge on conditioned Na-montmorillonite in 0.03 M  $\text{NaClO}_4$

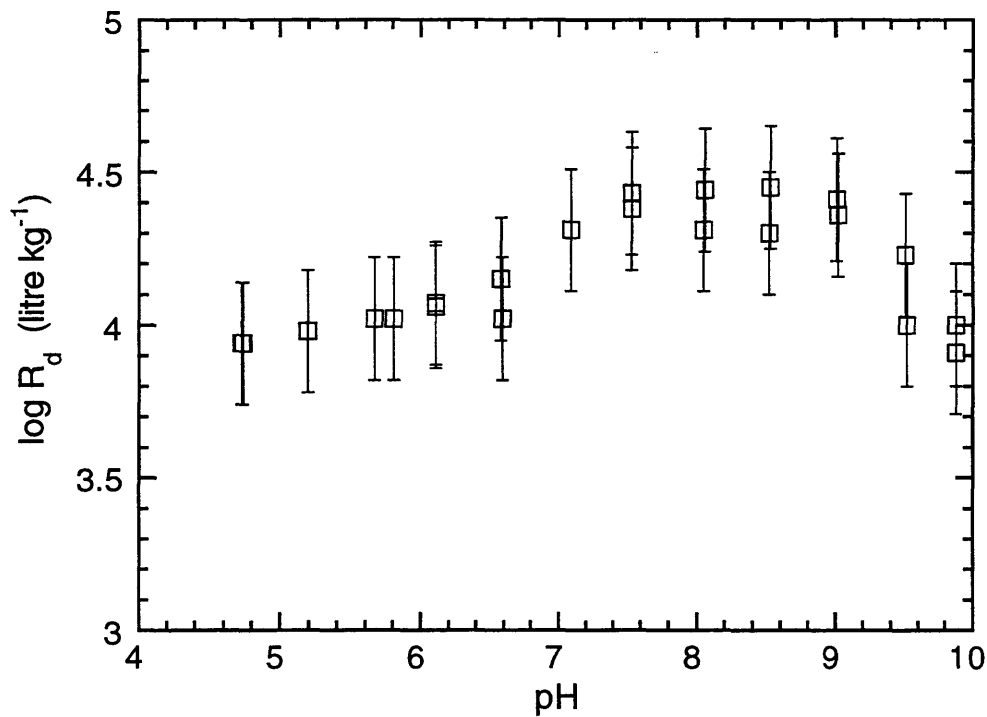


Figure 12: Ni sorption edge on conditioned Na-montmorillonite in 0.01 M NaClO<sub>4</sub>

#### 4.4.2 Ni Sorption Isotherms

Six sets of Ni sorption isotherms were measured on conditioned Na-montmorillonite over the pH range 8.2 to 4.7. These data are given in Figures 13 to 18. The experimental conditions are summarised in Table 7.

Table 7: Experimental conditions for the Ni sorption isotherm measurements on conditioned Na-montmorillonite at 0.1 M NaClO<sub>4</sub>.

Experimental Conditions	Fig.13	Fig.14	Fig.15	Fig.16	Fig.17	Fig.18
pH	8.2	7.7	7.0	5.9	5.1	4.7
Buffers	TRIS	TRIS	MOPS	MES	AA	AA
S:L ratio (gram litre <sup>-1</sup> )	0.24	0.24	0.24	0.24	0.24	0.24
Time (days)	7	7	7	7	7	7
Nr. of measurements	22	12	12	24	12	12

As the pH decreases from 8.2 to 4.7, the series of Ni isotherms shown in Figures 13 - 18 clearly demonstrate the gradual transition from a non-linear sorption behaviour dominated by surface complexation to a regime of constant sorption controlled by cation exchange. Also, the data sets at each individual pH illustrate the general principle that the contribution of the surface complexation mechanism to the overall sorption tends to increase with increasing pH and decreasing equilibrium concentration of the sorbate whereas the reverse is true for cation exchange.

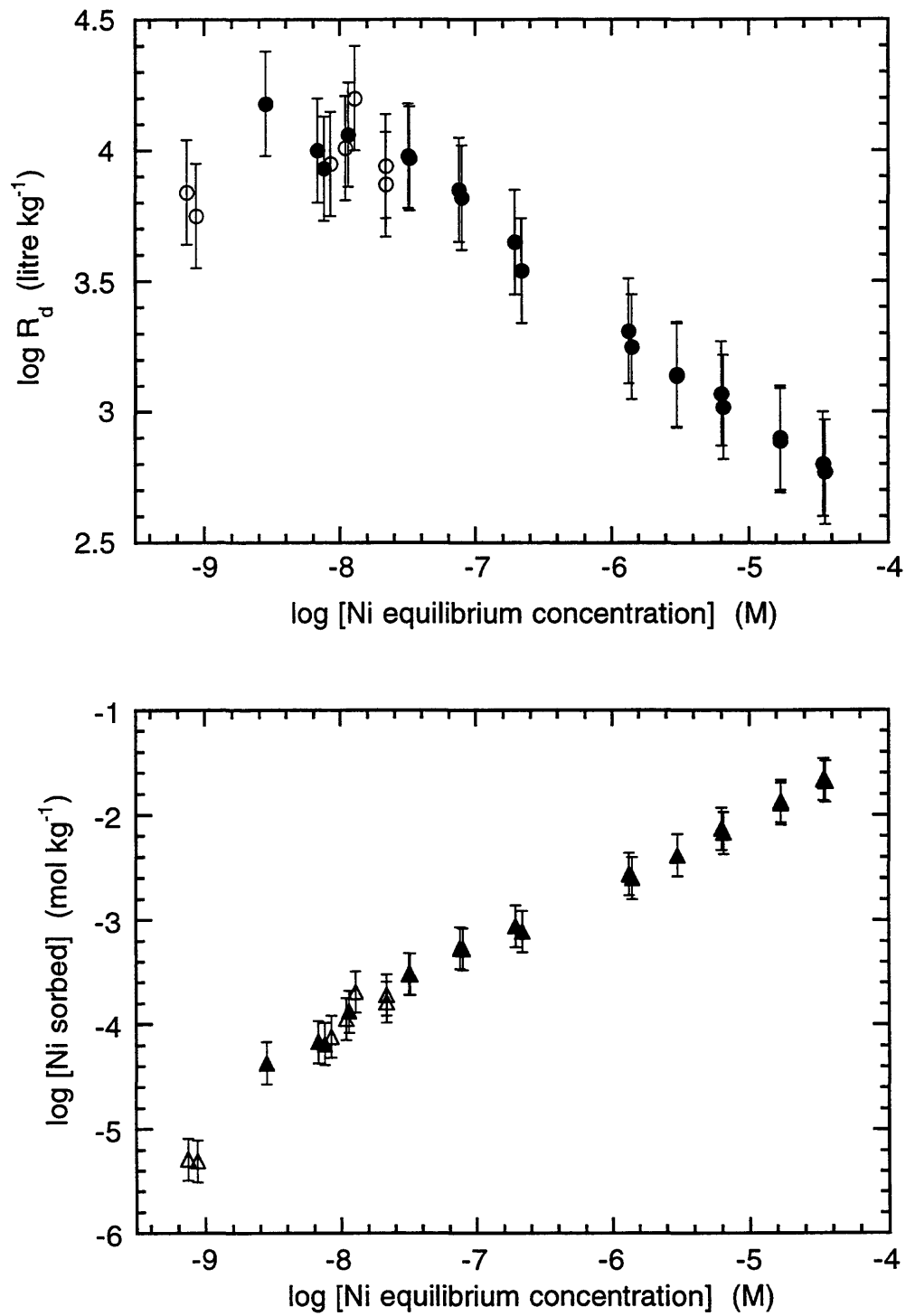


Figure 13: Ni sorption isotherm data on conditioned Na-montmorillonite at pH = 8.2 (Open symbols are data taken from Figure 10)

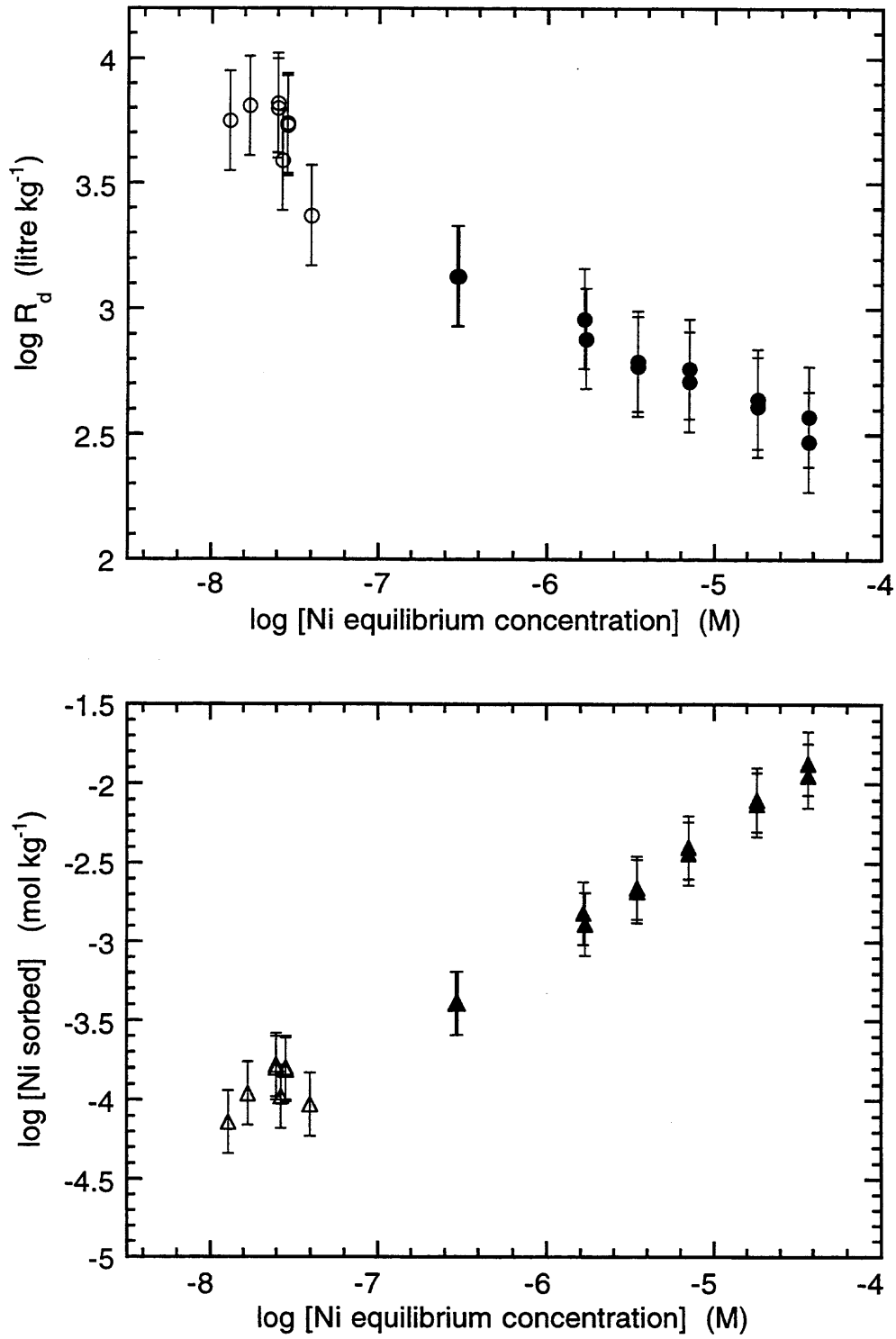


Figure 14: Ni sorption isotherm data on conditioned Na-montmorillonite at pH = 7.7 (Open symbols are data taken from Figure 10)

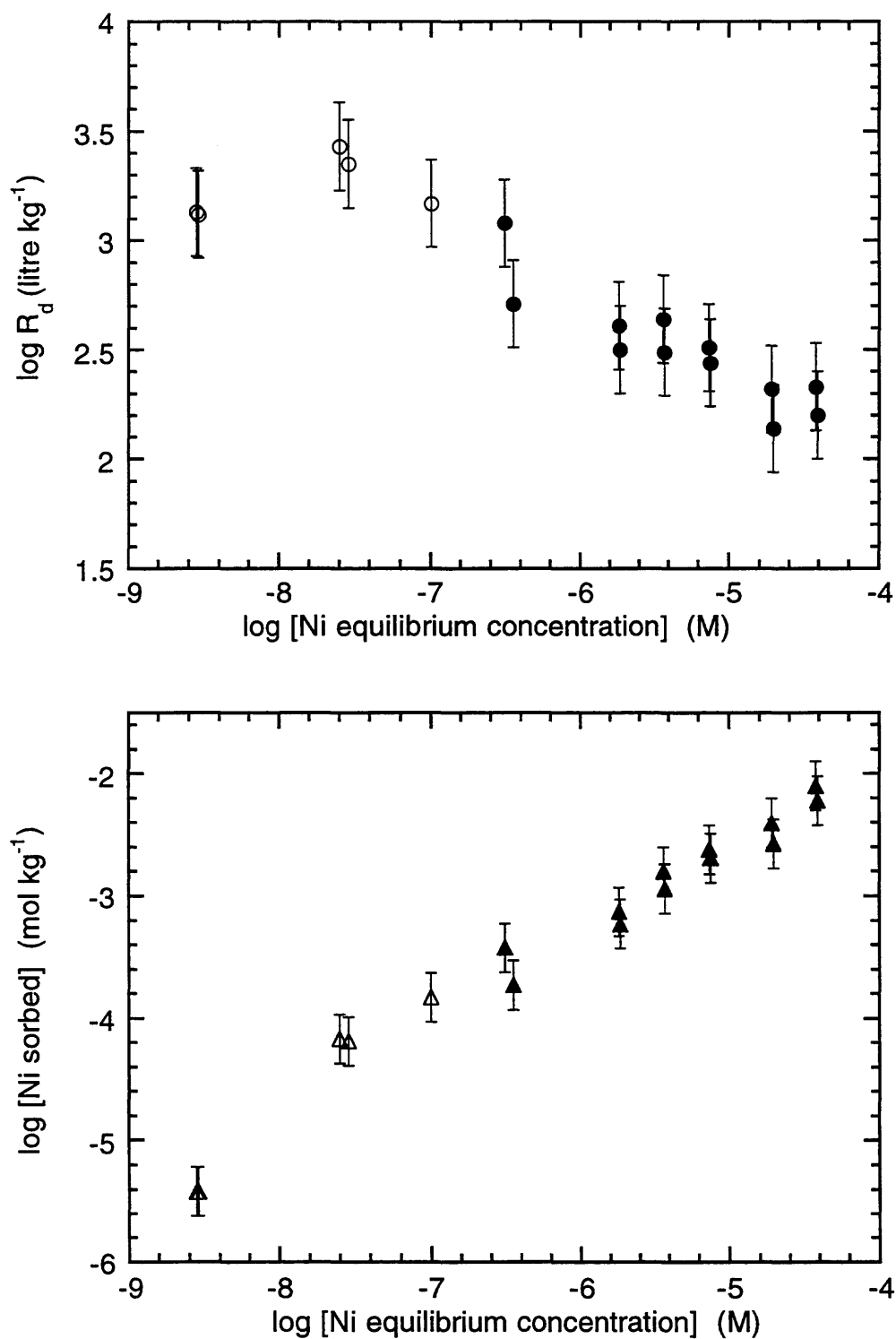


Figure 15: Ni sorption isotherm data on conditioned Na-montmorillonite at pH = 7.0 (Open symbols are data taken from Figure 10)

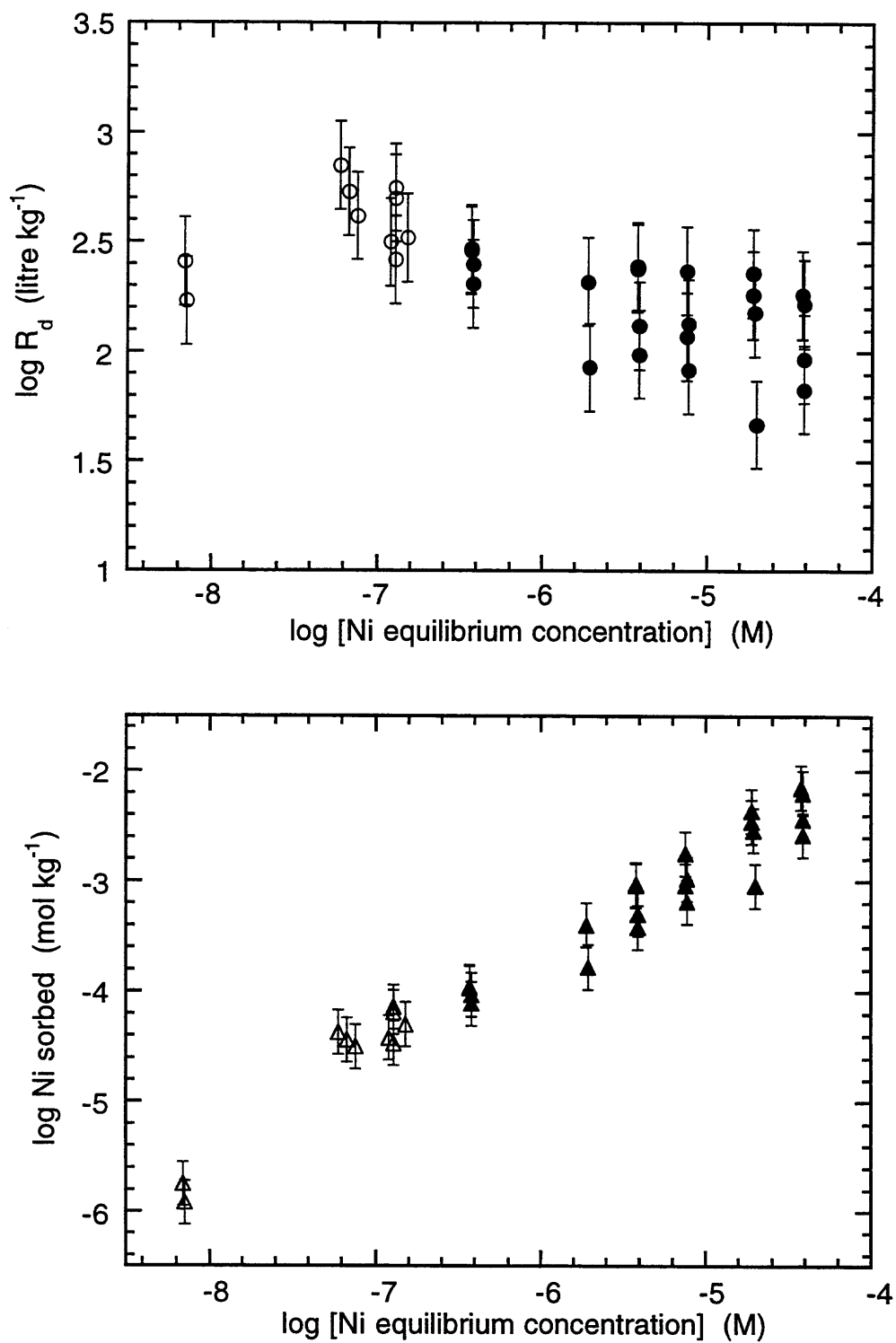


Figure 16: Ni sorption isotherm data on conditioned Na-montmorillonite at pH = 5.9 (Open symbols are data taken from Figure 10)

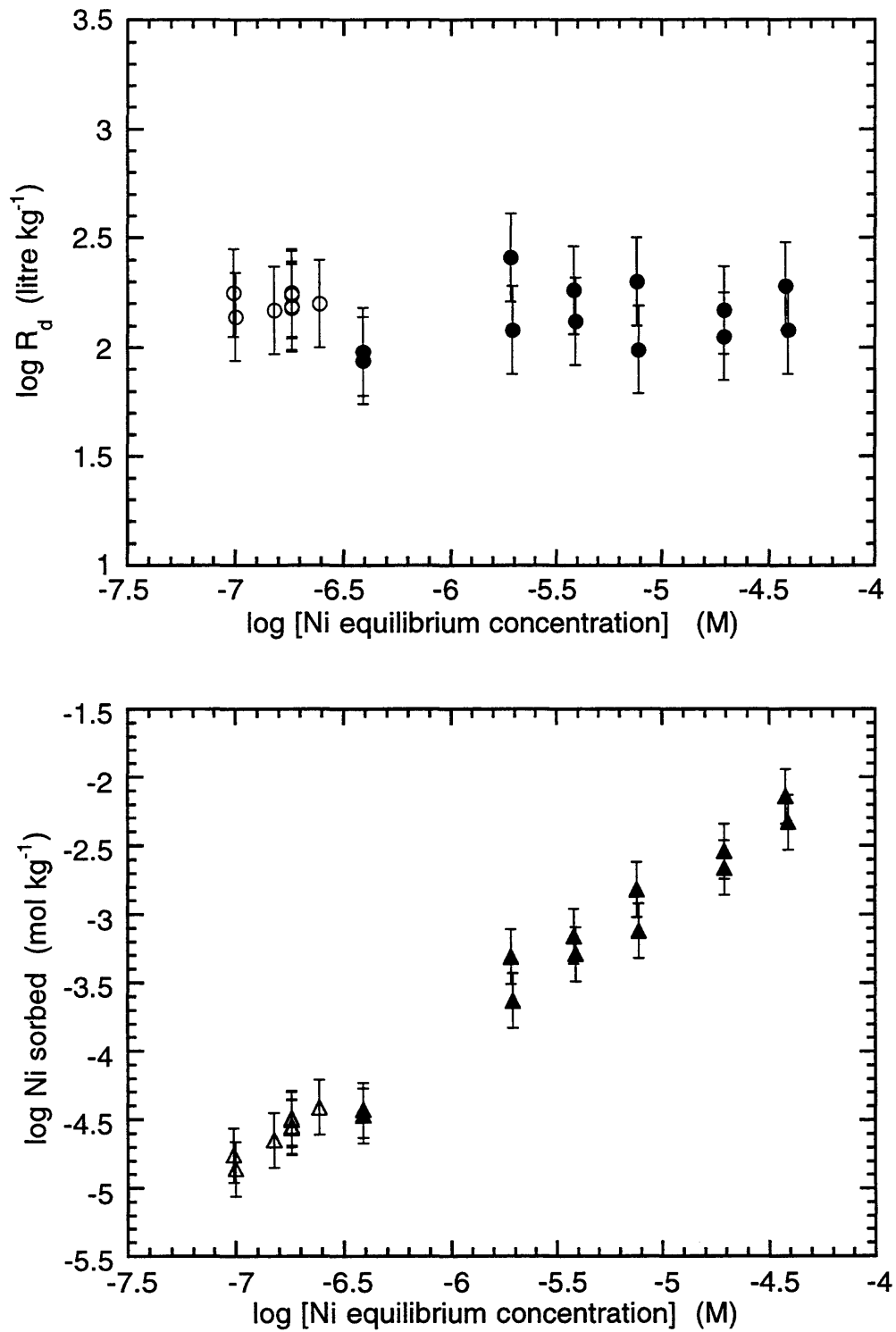


Figure 17: Ni sorption isotherm data on conditioned Na-montmorillonite at pH = 5.1 (Open symbols are data taken from Figure 10)

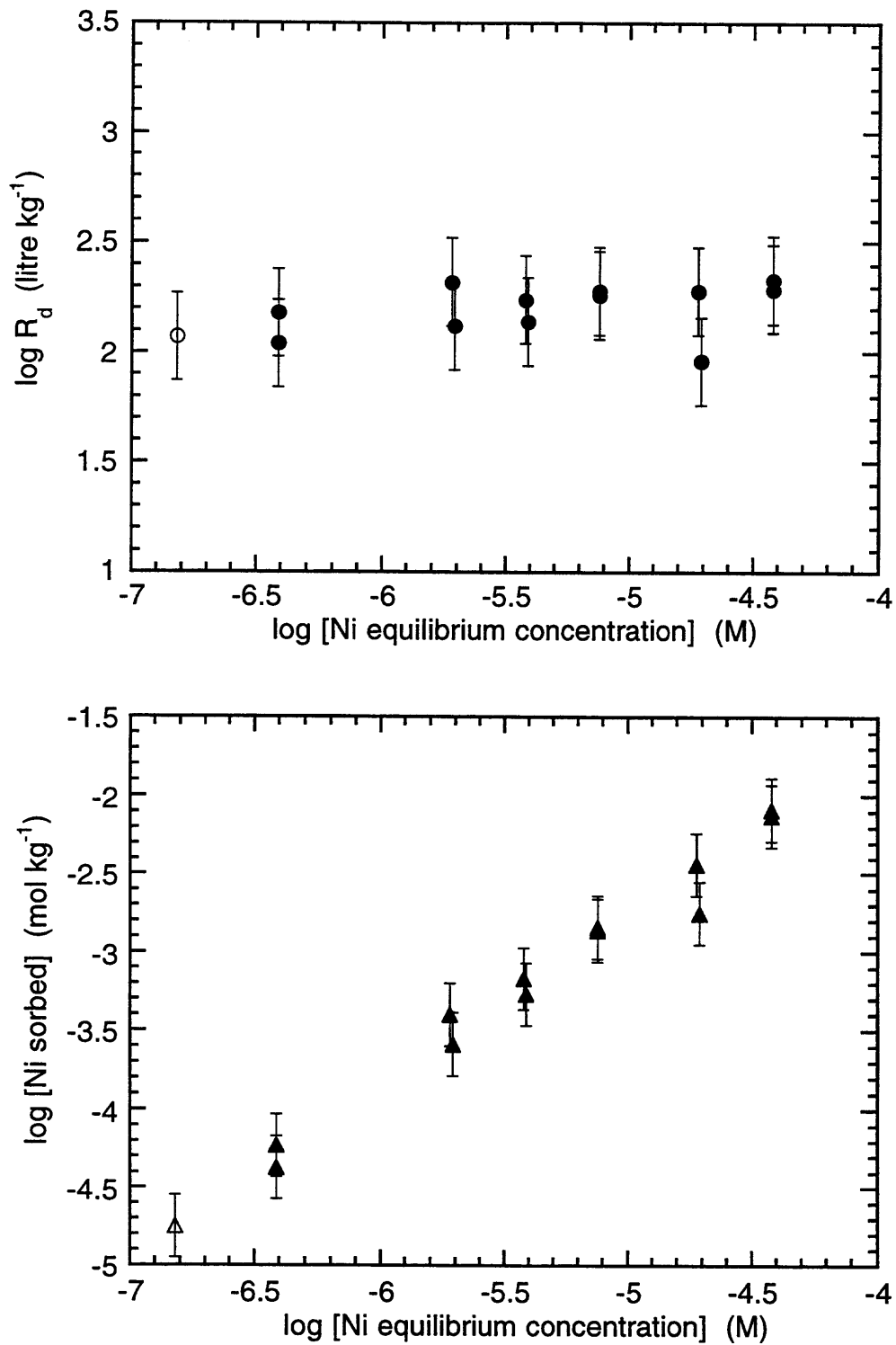


Figure 18: Ni sorption isotherm data on conditioned Na-montmorillonite at pH = 4.7 (Open symbols are data taken from Figure 10)

#### 4.5 Isotherms for Ca, Mg, Mn and Zn Deduced from Figures 1a-1d

In Part I, it was concluded that Ca, Mg, Mn and Zn were present in the system at fixed levels as sorbed cations on the conditioned Na-montmorillonite. These intrinsic inventories are summarised in Table 8.

Table 8: Intrinsic inventories of Ca, Mg, Mn and Zn in conditioned Na-montmorillonite

Nuclide	Intrinsic inventory (mol kg <sup>-1</sup> )
Ca	10 <sup>-3</sup>
Mg	3 x 10 <sup>-3</sup> - 6 x 10 <sup>-3</sup>
Mn	4 x 10 <sup>-4</sup>
Zn	10 <sup>-3</sup>

If the inventory and equilibrium concentrations as a function of pH are known, then the distribution ratio,  $R_d$ , can be calculated from a mass balance equation i.e.

$$m \cdot I_{RN} = m \cdot R_d \cdot C_{eq.} + V \cdot C_{eq.} \quad [4]$$

where  $I_{RN}$  is the intrinsic inventory of the nuclide, RN, expressed in mol kg<sup>-1</sup>. The other symbols have the same meaning as defined for equation 3, section 5.2.2.

Equation 4 has been used in conjunction with the concentration versus pH data in Figures 1 (a) to (d) and the intrinsic inventories given in Table 8 to calculate the sorption edges for Ca, Mg, Mn and Zn in 0.5 M NaClO<sub>4</sub> presented in Figures 19 (a) to (d) respectively. Where aqueous concentrations approach values corresponding to the inventories, the uncertainties associated with the calculated distribution ratios become very large, and such values have not been included in the plots. Sorption edges deduced indirectly from aqueous analysis data are clearly less accurate than those measured directly using radiotracers. However, they provided a useful additional source of data for extending the scope of the modelling studies.

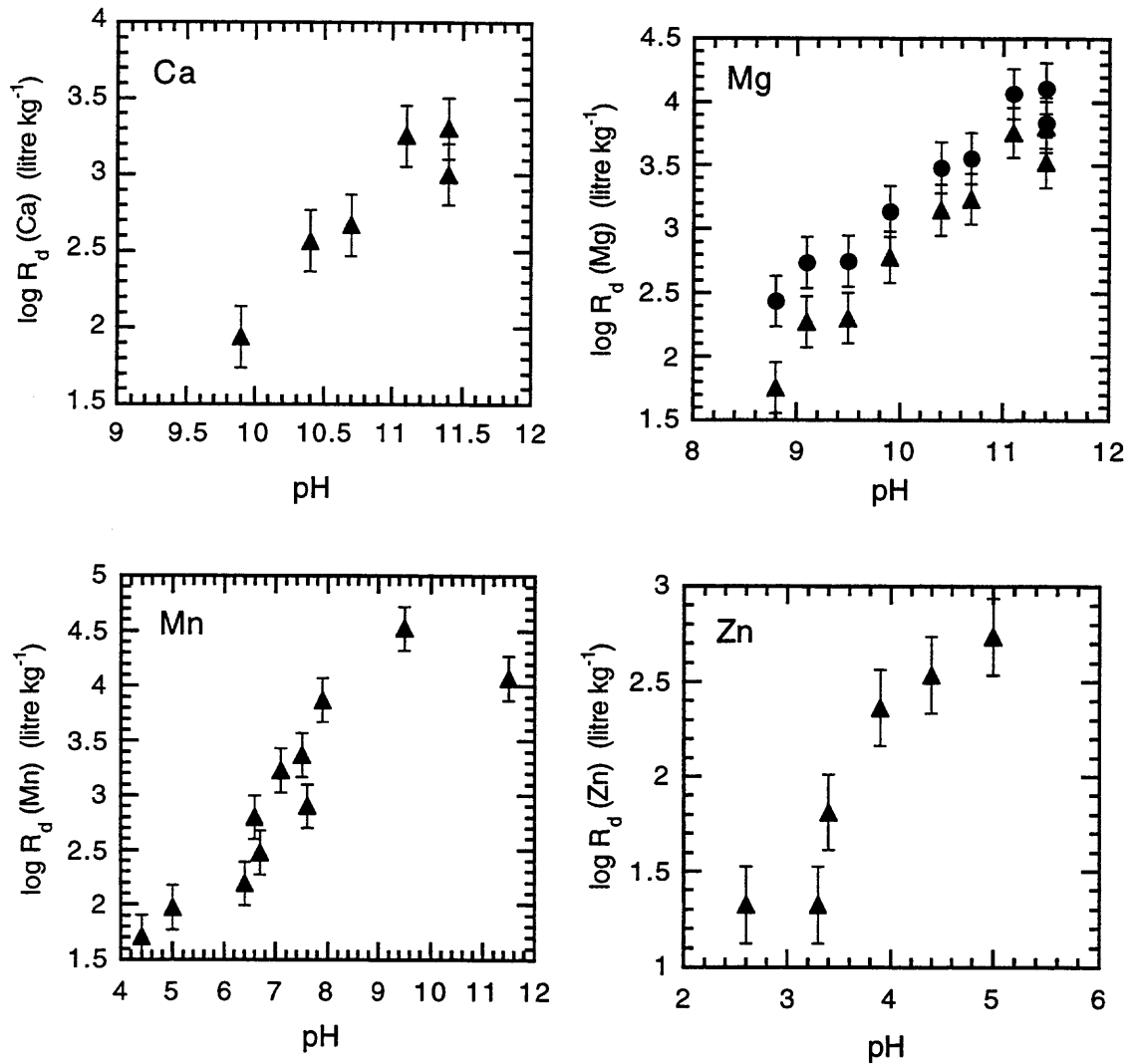


Figure 19: (a)-(d): Sorption edges for Ca, Mg, Mn and Zn deduced from aqueous analysis data, Figures 1 (a)-(d), using equation 4

## 5 CATION EXCHANGE

### 5.1 Background

The sorption data given in the previous chapter are modelled in some subsequent work (BRADBURY & BAEYENS 1995) using a code which calculates the overall sorption due to cation exchange and surface complexation mechanisms simultaneously. The report concentrates mainly on the surface complexation component since sorption by cation exchange and its incorporation into geochemical codes was covered in an earlier publication (BRADBURY & BAEYENS 1994). In order that the parameters values characterising the sorption by cation exchange are available for the modelling, we propose to derive them here.

If the general case of a cation B, valence  $z_B$ , in the aqueous phase exchanging with cation A, valence  $z_A$ , bound to the clay mineral surface is considered, the exchange reaction can be written as follows:



Cation exchange reactions are considered to be reversible, fast and stoichiometric. A mass action relation is normally used to describe the reaction in terms of a so-called selectivity coefficient. We have chosen to follow the definition of GAINES & THOMAS (1953) and accordingly define a stoichiometric selectivity coefficient,  ${}^B_A K_C^I$ , for equation 5 as:

$${}^B_A K_C^I = \frac{N_B^{z_A}}{N_A^{z_B}} \cdot \frac{[A]^{z_B}}{[B]^{z_A}} \quad [6]$$

[A] and [B] are the solution concentrations in mol litre<sup>-1</sup> of cations A and B respectively.  $N_A$  and  $N_B$  are equivalent fractional occupancies defined as the equivalents of A (or B) sorbed per unit mass divided by the cation exchange capacity (CEC), also expressed in equivalents per unit mass, which is taken to be constant.

One method of determining selectivity coefficients is via sorption measurements. If we define a sorption coefficient,  ${}^B R_{CE}$ , for the sorption of cation B by cation exchange as:

$${}^B R_{CE} = \frac{\text{Moles of } B \text{ sorbed by cation exchange per unit mass}}{\text{Moles of } B \text{ in aqueous solution per unit volume}} \quad [7]$$

or,

$${}^B R_{CE} = N_B \cdot \frac{CEC}{Z_B} \cdot [B]^{-1} \quad [8]$$

then,

$$N_B = {}^B R_{CE} \cdot \frac{Z_B}{CEC} \cdot [B] \quad [9]$$

For a bi-ionic system where one of the cations, B, is present at trace levels, we can take  $N_A \sim 1$ , and equation 6 simplifies to :

$${}^B K_C^A = N_B^{Z_A} \cdot \frac{[A]^{Z_B}}{[B]^{Z_A}} \quad [10]$$

Substituting the expression for  $N_B$  from equation 9 into equation 10 yields a general expression relating the selectivity coefficient,  ${}^B K_C^A$ , to the distribution ratio for cation B,  ${}^B R_{CE}$ , i.e.,

$${}^B K_C^A = Z_B^{Z_A} \cdot ({}^B R_{CE})^{Z_A} \cdot \frac{1}{(CEC)^{Z_A}} \cdot [A]^{Z_B} \quad [11]$$

Since cation exchange sites are local negative surface charges which arise as a result of isomorphic substitution of lattice cations (see for example GRIM 1953, VAN OLPHEN 1963), the density of these sites is not influenced by changes in pH and hence one of the main characteristics of sorption by cation exchange is its pH independence. Generally low pH and/or high nuclide

concentrations tend to favour cation exchange over surface complexation processes.

## 5.2 Selectivity Coefficient Values for Zn, Ca and Ni

The sorption edge plots for Zn, Ca and Ni (see chapter 4) were typified by a initial constant  $R_d$  region at low pH, followed by a strong increase in sorption as a function of pH. In this early plateau region, whose extent is nuclide and experimental condition dependent, the sorption is interpreted as being dominated by cation exchange. Hence, if the CEC of conditioned Na-montmorillonite is known, selectivity coefficients can readily be calculated from equation 11. (A CEC value of  $870 \pm 35 \text{ meq kg}^{-1}$  was measured for conditioned Na-montmorillonite in Part I.)

In order to provide additional evidence for our interpretation that the constant sorption observed at low pH values is dominated by cation exchange, Ni and Ca sorption edges were measured as function of  $\text{NaClO}_4$  concentrations, see previous chapter. If a bivalent monovalent system such as Ni-Na is taken as an example, and  $\frac{Ni}{Na}K'_C$  is assumed constant, then equation 11 can be re-arranged and expressed in a logarithmic form as:

$$\log(NiR_{CE}) = -2 \log[\text{NaClO}_4] + \log\left(\frac{1}{2} \frac{Ni}{Na} K'_C \cdot CEC\right) \quad [12]$$

Equation 12 indicates that when the sorption process for a bivalent cation is dominated by cation exchange with a monovalent cation, then a plot of  $\log NiR_{CE}$  against  $\log [\text{NaClO}_4]$  should have a slope of -2. Such plots are shown in Figures 20 and 21 for Ni and Ca. The slopes from a least squares analysis of the Ni and Ca data are -1.9 and -2.1 respectively. Both of these values are very close to -2 which supports the interpretation given above (see also SHIAO et al. 1979).

Key experimental data for the Ni, Zn and Ca sorption tests are summarised in Table 9 together with stoichiometric selectivity coefficients calculated as a function of  $\text{NaClO}_4$  concentration using equation 11.

Table 9: Calculated selectivity coefficients for Ni-Na, Ca-Na and Zn-Na exchange from experimentally measured sorption data

Cation	Data set from:	NaClO <sub>4</sub> (M)	pH range	log RCE (litre kg <sup>-1</sup> )	$\frac{B}{Na}K_c$	$\gamma_{Na}^*$	$\gamma_B^*$	$\frac{B}{Na}K_c$ (I=0)
Ni	Fig. 10	0.1	<4.5	1.9	2.0	0.78	0.37	3.3
	Fig. 11	0.03	<5.0	3.0	2.2	0.85	0.52	3.1
	Fig. 12	0.01	<6.0	4.0	2.4	0.9	0.66	2.9
	Single R <sub>d</sub>	0.003	<7.0	4.8	1.3	0.94	0.79	1.5
Ca	Single R <sub>d</sub>	0.267	6.2	1.1	2.1	0.74	0.29	4.0
	Fig. 8	0.1	<7.0	2.1	3.0	0.78	0.37	4.9
	Fig. 9	0.03	<8.0	3.1	2.7	0.85	0.52	3.8
	Fig. 9	0.01	<9.0	4.1	3.0	0.90	0.66	3.7
Zn	Fig. 5	0.1	<3.0	2.0	2.4	0.78	0.37	3.9

\*Activity coefficients were calculated using the Davies equation (Davies 1962).

"B" represents the bivalent cation.

The selectivity coefficient values,  $\frac{B}{Na}K_c$ , given in the above table are generally in good agreement with the (limited) literature data available. They are summarised below in Table 10.

Table 10: Selectivity coefficients for Zn-Na, Ni-Na and Ca-Na exchange on montmorillonite.

Cation B	$\frac{B}{Na}K_c$	Reference
Zn	3.9	This work (Table 9)
	3.6	MAES 1973
	3.7	MAES et al. 1976
Ni	3.1 ±0.2	This work (Table 9)
	3.2	MAES 1973
	3.7	MAES et al. 1976
Ca	4.1 ±0.5	This work (Table 9)
	3.4/3.9	VAN BLADEL et al. 1983
	3.7	MAES & CREMERS 1977
	3.4	SPOSITO et al. 1983

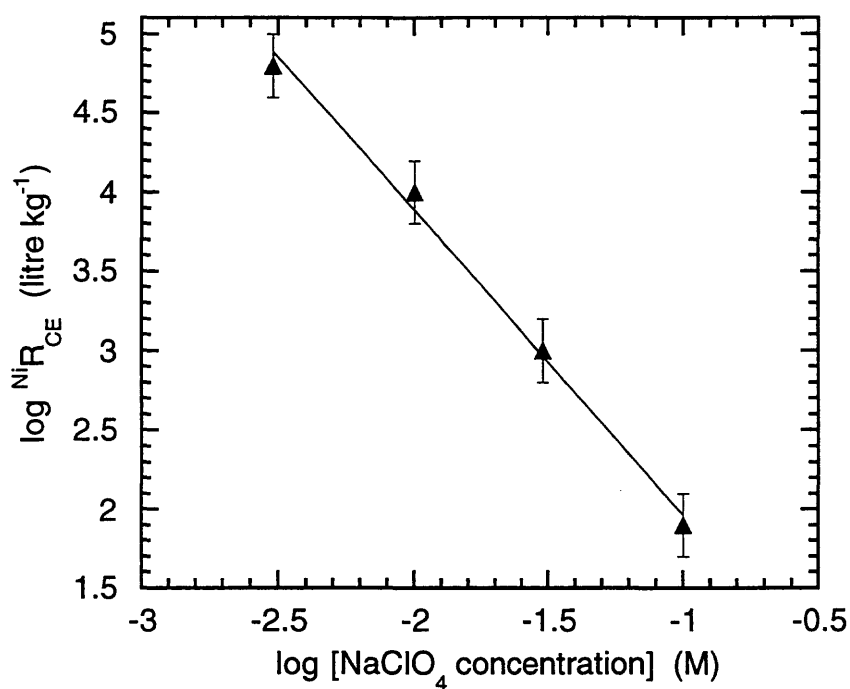


Figure 20: Sorption of Ni at trace concentrations on conditioned Na-montmorillonite as a function of NaClO<sub>4</sub> concentration. The continuous line is a least squares fit with a gradient of -1.9

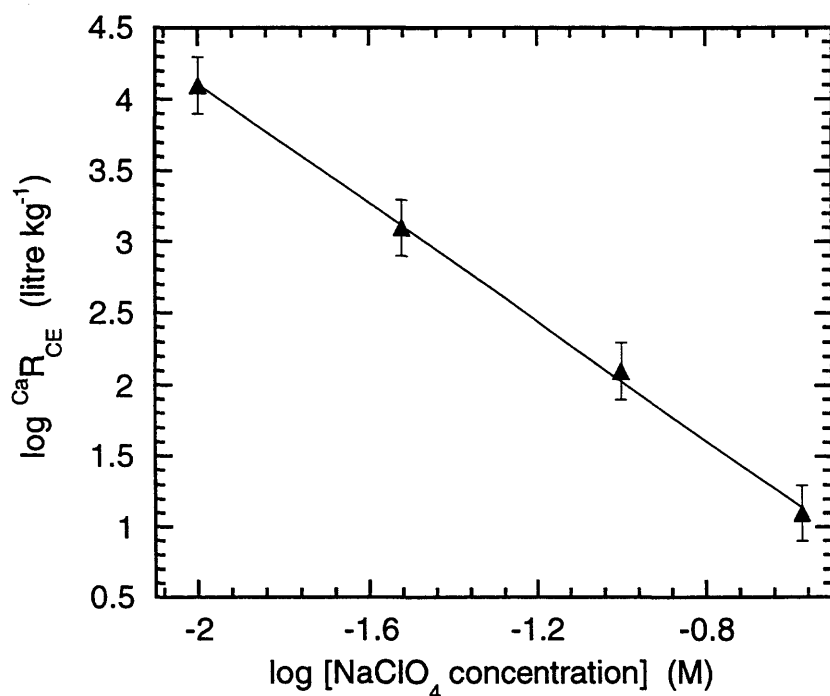


Figure 21: Sorption of Ca at trace concentrations on conditioned Na-montmorillonite as a function of NaClO<sub>4</sub> concentration. The continuous line is a least squares fit with a gradient of -2.1

## 6 CONCLUDING REMARKS

Sorption data, presented in the form of sorption edges and isotherms, have been measured over a wide variety of conditions (pH, ionic strength, S:L ratio, radionuclide concentration/inventory etc.) for Ni, Zn and Ca on conditioned Namontmorillonite. Zn, identified as an important background impurity in Namontmorillonite, and Ca, present in almost all natural systems, can potentially influence the sorption of other radionuclides, and, primarily for these reasons, were investigated in detail.

The form of the sorption edges suggested that two mechanisms were dominating the sorption behaviour. One was identified as cation exchange where the sorption is linear and pH independent. The exchange reactions are characterised by selectivity coefficients and these were determined for Ni, Zn and Ca yielding average values in the NaClO<sub>4</sub> concentration range from 0.01 to 0.1 of  $\frac{Ni}{Na}K_c \sim 3.1$ ;  $\frac{Ca}{Na}K_c \sim 4.1$  and  $\frac{Zn}{Na}K_c \sim 3.9$ .

The second mechanism which exhibited a strong pH dependency and non-linear sorption will be interpreted in Part III in terms of a surface complexation model. The sorption isotherm results, particularly those for Ni, strongly suggested that sorption was occurring on at least two types of pH dependent sites. At low radionuclide concentrations the sorption, expressed in terms of distribution ratios, was high and linear and occurred on a relatively small number of sites with a high binding affinity; "strong sites". For intermediate concentrations the sorption was non-linear, suggesting that sorption was taking place on an additional set of sites of greater concentration but having weaker binding constants; "weak sites". At still higher concentrations, the sorption again tended towards a linear behaviour but this time controlled by cation exchange.

One interesting and informative means of summarising the wide range of measurements described in the text is via a semi-quantitative sorption diagram such as the one shown in Figure 22 for Ni. The contributions to the overall sorption of the cation exchange (CE) and surface complexation (SC) mechanisms can be deconvoluted. The SC contribution is depicted in the diagram by strong continuous lines as a function of pH. (Sorption due to this

mechanism is not dependent on the concentration of the NaClO<sub>4</sub> background electrolyte.) The maximum quantity of Ni sorbed by this mechanism corresponds to the ≡SOH site capacity i.e.  $\sim 8 \cdot 10^{-2} \text{ mol kg}^{-1}$  (Part I, section 7.5), and is represented by the dot dashed line in Figure 22.

The sorption due to cation exchange is linear, independent of pH but strongly dependent on ionic strength. The strong dashed lines in Figure 22 have been calculated using the measured Ni-Na selectivity coefficients. For this mechanism the upper bound for the maximum quantity sorbed corresponds to the CEC of conditioned Na-montmorillonite i.e.  $\sim 0.43 \text{ mol Ni per kg}$  (dotted line in Figure 22).

Other bounding values can also be introduced. The finely dashed lines correspond to the solubility limits of Ni(OH)<sub>2</sub> (taken as the solubility controlling phase) at the pH values indicated. On the low concentration side, the natural background concentration of Ni in the system (an arbitrarily chosen value of  $10^{-9} \text{ M}$  is taken here as an example) provides the bound on the possible sorption values of Ni. Although this diagram can be used to make semi-quantitative predictions for Ni sorption in the Na-montmorillonite/NaClO<sub>4</sub> system, its main purpose is to pictorially summarise the data and illustrate how sorption values for Ni are constrained. Clearly, as will be shown in the modelling work, (BRADBURY & BAEYENS 1995) sorption models, incorporated in geochemical speciation codes are an entirely more satisfactory and efficient measure of predicting sorption values.

The data presented here, and in Part I, provide an extensive and varied data base for the modelling exercise. We would argue that when any system is being studied for the first time a similar effort to that described in Parts I and II is necessary. It should not be forgotten that independent data sets, other than those required for fitting, are required to test the validity of the model and parameter sets. Once the basic modelling parameter sets have been fixed, the experimental effort required to characterise the sorption of subsequent radionuclides in terms of their CE and SC parameters is considerably less.

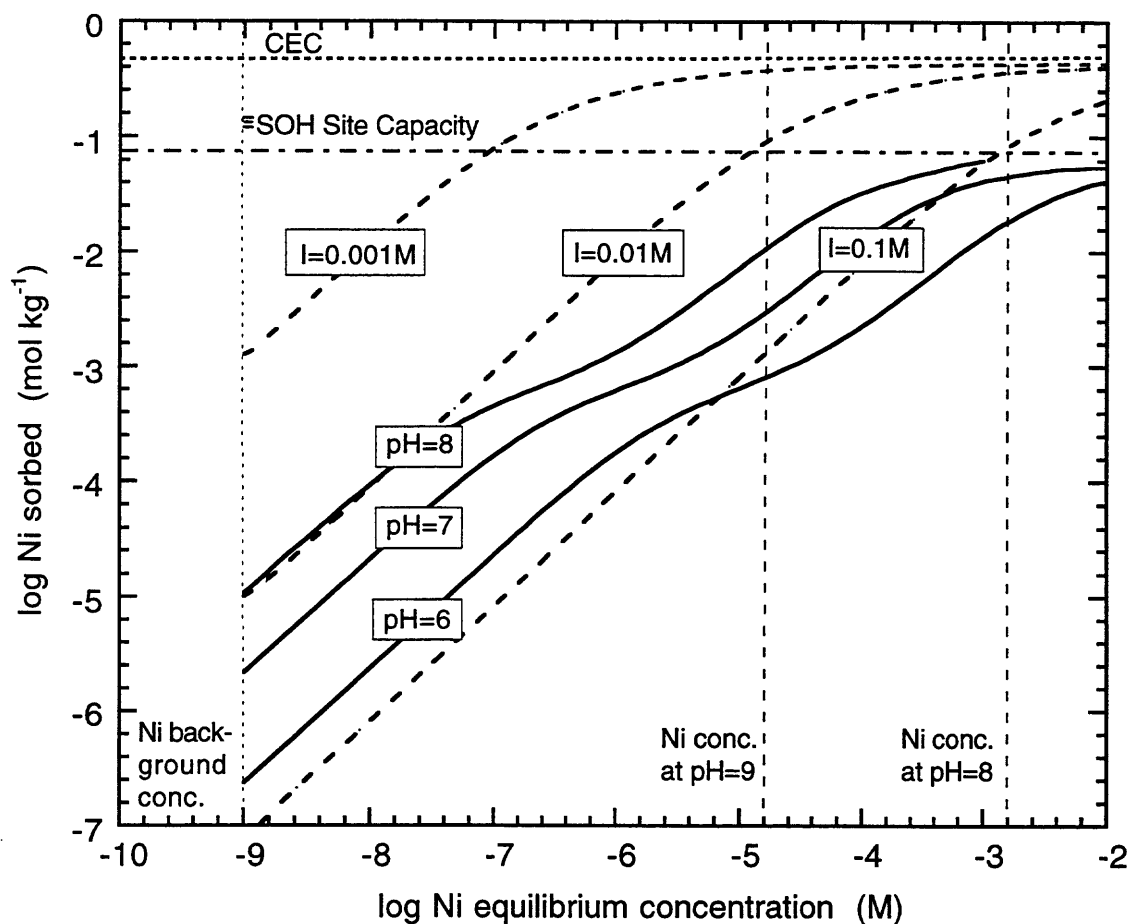


Figure 22: Diagrammatic representation of Ni sorption on Na-montmorillonite as a function of pH, ionic strength ( $\text{NaClO}_4$  concentration), and Ni equilibrium concentration.

———— Contribution of surface complexation to sorption (The max. theoretical value given by the  $\equiv\text{SOH}$  site capacity )

----- Contribution of cation exchange sorption (The max. theoretical contribution corresponds to the CEC)

Note that the overall sorption is given by the sum of the cation exchange and surface complexation contributions for a given set of conditions.

Bounding concentrations are : Background Ni concentration and Ni solubility limits. (See text for details.)

**ACKNOWLEDGEMENTS**

M. Mantovani and S. Haselbeck carried out much of the experimental work and their contributions to this programme of work are gratefully acknowledged. Chemical analyses were carried out by R. Keil. Professor W. Stumm is warmly thanked for his critical and helpful comments on this work. Gratitude is expressed to Drs. U. Berner, E. Wieland and J. Hadermann (PSI) and Dr. I. Hagenlocher (Nagra) for the many interesting discussions and for reviewing the manuscript. Partial financial support was provided by Nagra.

**REFERENCES**

- BAEYENS, B & BRADBURY, M.H. (1995): A quantitative mechanistic description of Zn, Ca and Ni sorption on Na-montmorillonite Part I: Physico-chemical characterisation and titration measurements. PSI Bericht Nr.95-10, Paul Scherrer Institut, Villigen, Switzerland and Nagra Technical Report NTB 95-04, Nagra, Wettingen, Switzerland.
- BRADBURY, M.H. & BAEYENS, B. (1995): A quantitative mechanistic description of Zn, Ca and Ni sorption on Na-montmorillonite Part III: Modelling. PSI Bericht Nr.95-12 Paul Scherrer Institut, Villigen, Switzerland and Nagra Technical Report NTB 95-06, Nagra, Wettingen, Switzerland.
- BRADBURY, M.H. & BAEYENS, B. (1994): Sorption by cation exchange: Incorporation of a cation exchange model into geochemical computer codes. PSI Bericht Nr.94-07, Paul Scherrer Institut, Villigen, Switzerland. Nagra Technical Report NTB 94-11, Nagra, Wettingen, Switzerland.
- DAVIES, C.W. (1962): Ion association. Butterworths, London.
- DZOMBAK, D.A., & MOREL, F.M.M. (1990): Surface complexation modelling. John Wiley & Sons, New York.
- GRIM, R.E. (1953): Clay mineralogy. Mc Graw Hill, New York.
- MAES, A. (1973): Ion exchange of some transition metal ions in montmorillonite and synthetic faujasites. Ph.D. Thesis, Catholic University Leuven.
- MAES, A. & CREMERS, A. (1977): Charge density effects in ion exchange. Part 1. Heterovalent exchange equilibria. J. Chem. Soc., Faraday Trans. I 73, 1807-1814.
- MAES, A., PEIGNEUR, P. & CREMERS, A. (1976): Thermodynamics of transition metal ion exchange in montmorillonite. Proc. Int. Clay Conf. 1975, 319-329.

- PERRIN, D. D. & DEMPSEY, B. (1974): Buffers for pH and metal ion control. Chapman and Hall, London.
- PEARSON, JR. F.J., BERNER, U. & HUMMEL, W. (1992): Nagra thermochemical data base II. Supplemental Data 05/92. Nagra Technical Report NTB 91-18, Nagra, Wettingen, Switzerland.
- VAN BLADEL, R., GAVIRIA, G. & LAUDELOUT, H. (1972): A comparison of the thermodynamic double layer theory and experimental studies on the Na-Ca equilibria in clay water systems. Proc. Int. Clay Conf. 1972, 385-398.
- VAN OLPHEN, H. (1963): An introduction to clay colloid chemistry. Interscience Publ., New York.
- SHIAO, S. Y. et al. (1979): Ion exchange equilibria between montmorillonite and solutions of moderate to high ionic strength. In: FRIED, S. (ed.) Radioactive waste in geological storage. ACS Symp. Series 100. Am. Chem. Soc.

